Geochimica et Cosmochimica Acta 335 (2022) 231–242

Contents lists available at ScienceDirect

Geochimica et Cosmochimica Acta

journal homepage: www.elsevier.com/locate/gca

Evolution of rare earth element and εNd compositions of Gulf of Mexico seawater during interaction with Mississippi River sediment

Segun B. Adebayo [a,*], Minming Cui [a,b], Thomas J. Williams [c], Ellen Martin [c], Karen H. Johannesson [a,d,e]

[a] Department of Earth and Environmental Sciences, Tulane University, New Orleans, LA 70118, USA
[b] Morton K. Blaustein Department of Earth and Planetary Sciences, Johns Hopkins University, Baltimore, MD 21218, USA
[c] Department of Geological Sciences, University of Florida, Gainesville, FL 32611, USA
[d] School for the Environment, University of Massachusetts Boston, Boston, MA 02125, USA
[e] Intercampus Marine Science Graduate Program, University of Massachusetts System, Boston, MA 02125, USA

ARTICLE INFO

Article history:
Received 6 February 2022
Accepted 22 August 2022
Available online 28 August 2022
Associate editor: Noah J. Planavsky

Keywords:
Rare earth elements
Neodymium isotopes
Sediment dissolution
Boundary exchange
Seawater

ABSTRACT

A closed-system batch reaction experiment was conducted for 270 days to evaluate the effects of interaction between Gulf of Mexico (GOM) seawater and Mississippi River sediments on the system's dissolved rare earth elements (REE) concentrations and neodymium isotopic compositions (εNd). This study specifically focuses on geochemical reactions involving silicic sediments derived from weathering of the North American continent as they affect the REEs and εNd of seawater along continental margins, in contrast to previous studies that investigated the influence of basaltic rocks and sediments on REEs and εNd in the ocean. Our results show that the dissolution of labile phases of lithogenic Mississippi River sediments leads to an approximately 100-fold increase in dissolved REE concentrations within the first 33 days of the experiment. Secondary mineral precipitation appears to lower the REE concentrations between days 33 and 270 of the experiment, although seawater REE concentrations remain elevated compared to initial values. The two-way elemental transfer involving dissolution and precipitation results in a net increase by a factor of 24 ± 12 (mean ± 1σ) in the dissolved REE concentrations by the end of the experiment (i.e., day 270). The dissolved REE concentration maxima observed after 33 days of the experiment represent the mobilization of approximately 0.37 % of the REE content of the operationally defined "exchangeable" fraction of the riverine sediments. The εNd values of the reactive lithogenic components were −9.77 and −9.95, which are similar to the GOM value of −9.81 ± 0.36. Because of the similarity between εNd values, changes in the seawater Nd isotope value throughout the experiment were subtle (mean ± std, reacted seawater εNd of −9.87 ± 0.17). The highest REE concentrations coincided with the most radiogenic εNd (-9.65 ± 0.23; day 33), which suggests that REE concentrations and εNd compositions of the GOM may be buffered by fluxes from sediments in the system. Our results are comparable to previous studies involving basaltic rocks and/or sediments of basaltic composition in that they demonstrate that silicic, river sediments are highly reactive in marine environments with regard to REE mobilization. The experimental results further suggest that "boundary exchange" plays an important role in influencing the εNd of seawater along continental margins dominated by large river systems, although the impacts of boundary exchange will be most profound where ambient seawater and river sediments have distinct Nd isotopic compositions (e.g., basaltic, or Precambrian shield material). Finally, our results indicate that the εNd value of GOM seawater is largely controlled by the lithogenic sediment delivered to the basin by the Mississippi River.

1. Introduction

Dissolved and/or particulate components from sources such as river water, groundwater, as well as diffusive fluxes from pore water and hydrothermal fluids, coupled with atmospheric depositions constitute the primary fluxes of trace elements to the ocean (Gaillardet et al., 1999, 2003; Haley et al., 2004; Viers et al., 2009; Oelkers et al., 2011; Abbott et al., 2019; Chevis et al., 2021). Among these potential sources, dissolved fluxes have been the focus of considerable research owing to the relative ease of mixing between their constituent trace elements and the ocean

* Corresponding author.
E-mail address: sadebay@tulane.edu (S.B. Adebayo).

https://doi.org/10.1016/j.gca.2022.08.024
0016-7037/

(Pearce et al., 2013). Atmospheric dust has also been a primary research target because of its importance in biogeochemical cycles, such as that for iron (e.g., Chester et al., 1993; Greaves et al., 1994; Boyd and Ellwood, 2010; Pavia et al., 2020). However, several studies have also demonstrated that the dissolution of suspended particulate materials (SPM) and labile fractions of lithogenic sediments within estuaries and/or on the continental shelf are important contributors of trace elements via benthic fluxes to the ocean (e.g., Haley et al., 2004; Arsouze et al., 2009; Jeandel et al., 2011; Jones et al., 2012a, 2012b; Oelkers et al., 2011; Pearce et al., 2013; Wilson et al., 2013). In the case of rare earth elements (REE), the benthic flux appears to be critical for resolving imbalances in modern marine mass balance models (Haley et al., 2004, 2017; Abbott et al., 2015a, 2015b; Abbott, 2019).

Riverine fluxes, which are among the dominant sources of particulate material to the ocean, contribute a combined global discharge of approximately 30 Gt/year from both suspended particles and bedload sediments (Walling 2006; Peucker-Ehrenbrink, 2009; Pearce et al., 2013). Interactions between seawater and lithogenic sediments and/or SPM are reported to be important to seawater chemistry in nearshore environments through a process referred to as "boundary exchange" (Lacan and Jeandel, 2005; Arsouze et al., 2009; Jones et al., 2012a, 2012b; Pearce et al., 2013; Wilson et al., 2013; Abbott et al., 2015a). These researchers proposed that continental margins can function as fluidized bed reactors, where the interactions between SPM, sediments, and seawater through a combination of dissolution and precipitation can result in changes in the radiogenic isotope composition as well as trace element concentrations of seawater. For example, it is estimated that approximately 1–3 % of the lithogenic sediments carried by rivers and deposited offshore dissolve in seawater and release important amounts of trace elements to the ocean (Lacan and Jeandel, 2005; Arsouze et al., 2009; Jeandel et al., 2011; Rousseau et al., 2015).

Other studies have examined the boundary exchange processes through laboratory experiments involving seawater and lithogenic sediments (e.g., Oelkers et al., 2011; Jones et al., 2012a; Pearce et al., 2013; Wilson et al., 2013). These experimental studies also indicate that the dissolution of lithogenic sediments in seawater is coupled to precipitation of secondary minerals, which together can amount to small or even no net change in seawater trace element concentrations but may dramatically impact radiogenic isotope ratios in seawater when the dissolving lithogenic sediments have substantially different isotope compositions than the ambient seawater (e.g., Pearce et al., 2013; Jeandel and Oelkers, 2015). By this two-way mass transfer process (i.e., "boundary exchange") the Nd isotopic composition of seawater may be substantially altered while the Nd concentrations remain unchanged. Specifically, differences in isotopic composition between seawater and lithogenic sediments (i.e., εNd gradient), dissolution rates, and concentrations of Nd in seawater are all recognized as important factors contributing to the boundary exchange process (Oelkers et al., 2011; Jones et al., 2012a; Pearce et al., 2013; Wilson et al., 2013; Abbott et al., 2015b; Jeandel and Oelkers, 2015).

The evolution of REE concentrations and εNd of seawater during interactions with lithogenic sediments has been experimentally examined using relatively reactive lithogenic sediments of basaltic compositions (e.g., Jones et al., 2012a; Pearce et al., 2013; Wilson et al., 2013). Likewise, Oelkers et al. (2011) used data from Johnson et al. (2004) to show via batch reactor experiments that less than an hour was required for 1 g of basaltic material to alter the Nd isotopic composition of 1 kg of seawater. The dissolution rate of lithogenic sediments was reportedly affected by changes in the sediment/seawater ratio, temperature, surface area of the SPM/sediments, and the bulk chemical composition of sediments (e.g., basaltic glass; Gíslason and Oelkers, 2003; Oelkers et al., 2011). Studies of marine benthic fluxes reveal their importance as a source of REE during boundary exchange and have also expanded on and attempted to quantify the "source" component of the boundary exchange process (Abbott et al., 2015a, b,2019; Abbott, 2019). As with the case of lithologic sediment dissolution, for marine benthic fluxes to alter the Nd isotope composition of ambient seawater, the isotopic composition of the benthic source must be different from that of the overlying seawater (e.g., Wilson et al., 2013; Abbott et al., 2015a, 2022; Haley et al., 2017). Nonetheless, the results of several investigations of benthic fluxes are consistent with its importance as a component of boundary exchange processes that impact εNd in the ocean (e.g., Jones et al., 2012a; Pearce et al., 2013; Abbott et al., 2015b; Jeandel and Oelkers, 2015).

Both Jones et al. (2012a) and Pearce et al. (2013) reported rapid changes in the Nd concentrations and Nd isotopic compositions of seawater during interaction with basaltic particulate materials in batch reactors. The choice of basaltic particulate materials for these experiments reflects the relatively fast dissolution rate of basaltic materials (i.e., glass) relative to silicic/felsic materials and the fact that the ocean crust and ocean islands are chiefly composed of basalts (Oelkers and Gíslason, 2001; Dupré et al., 2003; Gíslason and Oelkers, 2003; Navarre-Sitchler and Brantley, 2007; Gudbrandsson et al., 2011; Oelkers et al., 2011). However, a major proportion of sediment fluxes to the ocean is from weathering of granitic to granodioritic continental rocks (Holeman, 1968). Continental sources of lithogenic sediments to shelf and slope regions are important globally including the North Atlantic where evidence of Nd isotopic "relabeling" of local seawater by reaction with silicic sediments has been documented (e.g., Roberts and Piotrowski, 2015; Howe et al., 2016; Blaser et al., 2020). Hence, it is also imperative to account for the impact of continental-derived, lithogenic sediments on the Nd isotope composition of seawater via boundary exchange processes, including benthic fluxes, to the geochemistry of the ocean.

Here, we explore the evolution of REE concentrations and the Nd isotope composition of seawater during reaction with silicic river sediments. We investigate whether the boundary exchange process previously reported from experiments in basaltic systems is also dominant in silicic systems. Specifically, we conducted a 270-day time-series, closed-system batch reaction experiment involving sediments from the Mississippi River and open-ocean seawater from the Gulf of Mexico (GOM). We monitored the dissolved REE concentrations and Nd isotope composition of the reacted seawater as a function of time to investigate the evolution of the dissolved REE and Nd isotope compositions.

2. Materials and methods

2.1. Study site

The Mississippi River was chosen in this study because it is the seventh-largest river in the world in terms of sediments discharge to the ocean (210 Mt/year; McKee et al., 2004). Hence, the silicic sediments in the Mississippi River system provide an ideal contrast to the basaltic sediments used in previous experimental studies that have explored the boundary exchange process (e.g., Jones et al., 2012a; Pearce et al., 2013). Likewise, Osborne *et al.* (2015) observed shifts in the Nd concentrations and Nd isotope composition of the GOM waters from west to east, suggesting the likelihood that continental sources impact the Nd isotopes variability within the GOM (e.g., Adebayo et al., 2018). Lastly, the Mississippi River delta is situated on a continental shelf that comprises approximately 33 % of the total area of the GOM (Trefry and Shokes, 1981; Adebayo et al., 2018) and provides a potential site for sub-

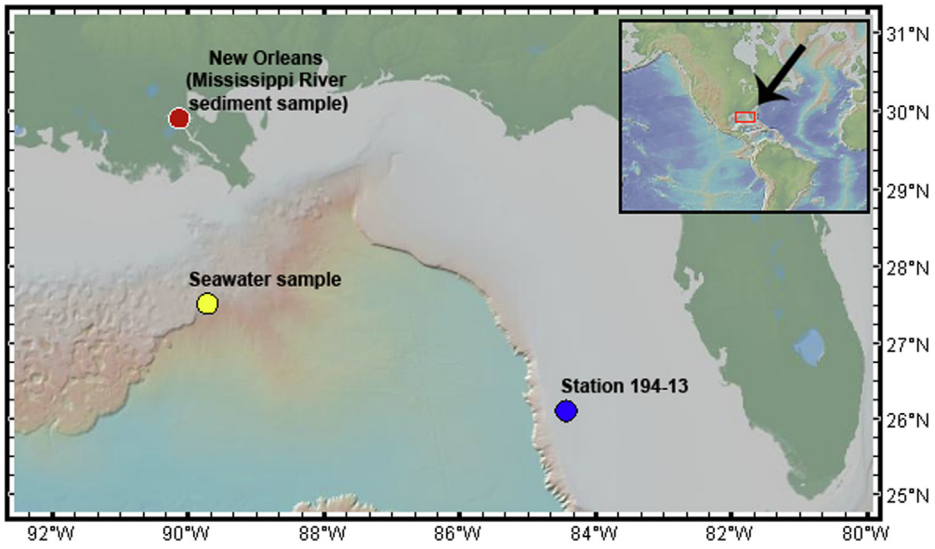

Fig. 1. Map showing the locations of the samples used in the batch reaction experiment. The sediment sample was collected at the Mississippi River bank in New Orleans (red dot), the seawater sample was collected in the Gulf of Mexico, and Station 194–13 from Osborne et al. (2014) was used for Nd isotope comparison. Base map from GeoMapApp. (For interpretation of the references to colour in this figure legend, the reader is referred to the web version of this article.)

stantial continent-ocean interactions including boundary exchange.

2.2. Sample collection

Sediment from the Mississippi riverbank in New Orleans was collected in October 2017 (Fig. 1). The sample (approximately 15 kg) was collected by grab sampling using a shovel at a location a few meters from the riverbank and transferred directly into ziplock® style polyethylene plastic bags. The bagged sediment sample was then transported to the laboratory where it was oven-dried at 40 °C and stored before use in the batch reaction experiment. Seawater was collected from the GOM during the ECOGIG, Point Sur 17–19 Cruise of April 13 – 18, 2017, aboard the 135 ft. R/V Point Sur vessel that is owned by the University of Southern Mississippi. The seawater was collected using water trapping bottles on CTD-rosette systems at a depth of 400 m (latitude 27.5297, longitude −89.7188; Fig. 1) and then emptied into trace metal grade acid pre-cleaned 50 L carboys. Upon arrival at Tulane University on 19 April 2017 (approximately 6 days after collection), the seawater sample was filtered through 0.45 μm pore size polyethersulfone membrane filters (Pall Corporation) to remove large particulate matter and plankton (Sholkovitz, 1992), acidified from the original pH of 8.2 to pH < 2 using ultrapure (Optima™ grade) HCl (12 M), and then stored at 4 °C until the commencement of the batch reaction experiments.

2.3. Sediment characterization

The physicochemical properties of the Mississippi riverbank sediment sample were investigated both before and after the batch reaction experiment. The surface features of individual grains in the sediments and elemental composition of grain coatings were determined by scanning electron microscopy (SEM) using a Hitachi 4800 High-resolution SEM with a 1.0 nm resolution at 15 kV (Fig. 2). The mineralogy of the sediments was further examined by X-ray diffraction (XRD, Scintag diffractometer, XDS 2000, Cu Kα, λ = 0.154 nm, U = 8.047 KeV, I = 38 mA) at a scanning rate of 1°/min. The XRD was equipped with a high-resolution solid-state detector and an automated sample changer (Fig. S1).

The REE concentrations in the operationally defined "exchangeable" fraction of Mississippi riverbank sediments were investigated

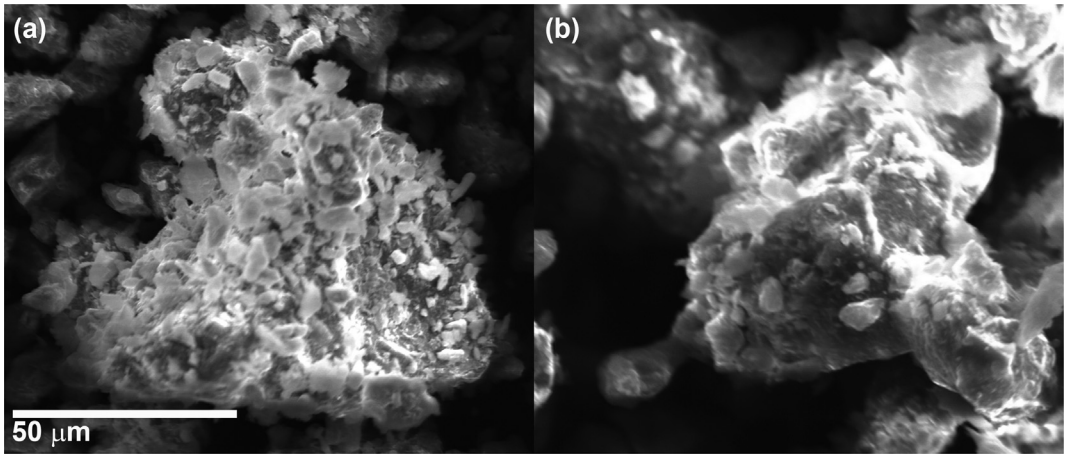

Fig. 2. Scanning electron microscopy (SEM) images of individual grains from the Mississippi River sediments. Panel (a) shows the surface morphology before, and panel (b) shows the surface morphology after the closed-system batch reaction experiment involving the sediments and Gulf of Mexico seawater.

using the sequential extraction procedure of Tessier et al. (1979) as described in Adebayo et al. (2018). The "exchangeable" fraction is largely derived from weakly adsorbed trace elements associated with clays, hydrated oxides of iron and manganese, and organic matter that can be impacted by changes in solution pH, ionic composition, and redox conditions (Tessier et al., 1979). Although Tessier et al. (1979) included extraction methods for other fractions, for a total of five fractions, we specifically targeted the "exchangeable" fraction because it is affected by changes in ionic strength that can occur in estuarine waters during river water-seawater mixing. (Results for the other four sequential extractions are provided in Adebayo et al., 2018).

Briefly, the extraction procedure consisted of one duplicate extraction of the riverbank sediments as follows: a 0.5 g (dry weight) aliquot of the sediments sample was leached with 8 mL of 1 M sodium acetate (CH_3COONa) at pH 8.2 and room temperature (23 ± 2 °C) in a 50 mL HDPE centrifuge tube under constant agitation for 1 h. The solution was then separated from the sediments by centrifugation at 3000 rpm for 20 min, after which the supernatant was collected into a 50 mL centrifuge tube, filtered through 0.45 μm pore size polyethersulfone membrane filters (Pall Corporation), acidified to pH < 2 with ultrapure HNO_3, and stored at 4 °C until analysis. Although sequential extractions methods are subject to possible artifacts from incomplete dissolution of target phases, non-selectivity of extractant, and re-adsorption, and should be viewed with caution, they can provide important insights into the distributions of trace elements in sediments (Tipping et al., 1985; Sholkovitz, 1989; Wilkin and Ford, 2002; Adebayo et al., 2018; Akintomide et al., 2021).

2.4. Batch reaction experiment

The closed-system batch reaction experiment was performed following an approach modified from Jones et al. (2012a) and Pearce et al. (2013). Before the batch experiment, the pH of the open ocean seawater sample was readjusted to 8.2 using 1 M Trace Metal™ grade NaOH. The batch reaction experiment was conducted at room temperature (23 ± 2 °C) over 270 days (9 months). Nine 6 L high-density polyethylene (HDPE) bottles were used as the reaction vessels to ensure that the ratio of the homogenous sediments to seawater remained unchanged after sampling throughout the experiment. Each batch reaction unit contained initial sediment to seawater ratios of 1:3.5 by weight (i.e., 1 kg sediments to 3.5 kg seawater) to ensure that sufficient Nd is present in the solution for isotopic determination (Jones et al., 2012a). The batch units were manually agitated at regular intervals throughout the experiment, daily for the first week, and then weekly for the remaining duration of the experiment.

Reaction progress was monitored by measuring pH and dissolved silica (Si) concentration from 10 mL water samples collected at regular intervals before agitation of the system and filtered through a 0.2 μm polyethersulfone membrane filters (Gelman Sciences). The pH measurements were made using a double-junction pH electrode calibrated with NIST traceable pH buffers (pH 4, 7, and 10) before each sampling event. The dissolved Si concentration was measured with a UV/VIS spectrophotometer (Hach DR 2800) following the silica HR silicomolybdate method with a detection limit of 0.01664 mmol kg^{-1} (Hach, 2007). At the end of each reaction period (i.e., Day 1, 2, 3, 6, 14, 33, 60, 120, and 270) as modified from Jones et al. (2012a), one batch reaction unit was "sacrificed" by collecting a 500 mL water sample for dissolved REE concentrations measurement and approximately a 2.5 L water sample for Nd isotope analysis. The samples were filtered through 0.45 μm pore size polyethersulfone membrane filters (Pall Corporation) to remove lithogenic sediment particles that may have been entrained during sample handling and then acidified to pH < 2 with ultra-pure HNO_3 (16 M) before storage at 4 °C until analysis. The filter sizes were selected following Pearce et al. (2013) to allow for a direct comparison of our results.

At the end of the batch reaction experiment, the dissolved REE concentrations in the reacted seawater were determined using a previously established method (Greaves et al., 1989; Johannesson et al., 2011, 2017; Chevis et al., 2015; Adebayo et al., 2018, 2020). Briefly, 30 mL aliquots of the filtered and acidified water samples were loaded onto Bio-Rad® Poly-Prep columns packed with approximately 2 mL of Bio-Rad® AG 50 W-X8 (200 – 400 mesh, hydrogen form) cation exchange resin. Similarly, 30 mL aliquots of the National Research Council Canada (Ottawa, Canada) Standard Reference Material (SRM) for estuarine waters (SLEW-3) and Millipore-Q water (18.2 MΩ cm), which acted as an analytical blank, were loaded onto identical columns (e.g., Johannesson et al., 2017). Before loading, the columns were pre-cleaned following the procedure reported by Georg et al. (2006). After loading the samples onto the columns, iron (Fe) and barium (Ba) were sequentially eluted by rinsing, first with 3 mL of 1.75 M ultra-pure HCl (Optima™ grade), followed by 3 mL of 2 M ultra-pure HNO_3 ((Optima™ grade; Greaves et al., 1989). Lastly, the REEs were eluted from the columns using 10 mL of 8 M ultrapure HNO_3 and collected into pre-cleaned Teflon® beakers. The REE eluents were subsequently evaporated to near dryness and then re-dissolved in 10 mL of 1 % (v/v) ultrapure HNO_3 solution. The resulting solution was then analyzed for REEs using HR-ICP-MS (i.e., Thermo Fisher Element 2) at Tulane University.

Before the instrumental analysis, each 10 mL concentrated aliquot was spiked with ^{115}In (at 1 μg kg^{-1}), as an internal standard. To minimize various polyatomic oxide/hydroxide and other mass interferences, multiple resolution configurations were used on the HR-ICP-MS (e.g., Chevis et al., 2015). The REE isotopes monitored at various resolutions are as follows: ^{139}La, ^{140}Ce, ^{141}Pr, ^{143}Nd, ^{145}Nd, ^{146}Nd, ^{147}Sm, ^{149}Sm, ^{151}Eu, ^{153}Eu, ^{155}Gd, ^{157}Gd, ^{158}Gd, ^{159}Tb, ^{161}Dy, ^{163}Dy, ^{165}Ho, ^{166}Er, ^{167}Er, ^{169}Tm, ^{172}Yb, ^{173}Yb, and ^{175}Lu, at low and high-resolution modes; ^{139}La, ^{140}Ce, ^{141}Pr, ^{143}Nd, and ^{145}Nd, at low and medium-resolution modes. We specifically monitored ^{151}Eu, ^{153}Eu, and the HREEs in high-resolution mode to resolve interferences from BaO^+ and $LREEO^+$ species formed in the plasma stream on the two Eu isotopes, and $LREEO^+$ and $MREEO^+$ species on the HREEs (e.g., see Johannesson and Lyons, 1994, 1995; Johannesson et al., 1997). A series of REE calibration standard solutions with concentrations 5, 10, 20, 100, 500, and 1000 ng kg^{-1} were prepared from NIST traceable High Purity Standards (Charleston, SC). All the reported REE concentrations are from five replicate analyses and show the instrument's precision (Table 1). Analytical precision for the REE analyses was always better than 5 % relative standard deviation (RSD), and analytical accuracy of the SRM SLEW-3 was typically within 5 % of the values reported by Lawrence and Kamber (2006). These procedures are consistent with Johannesson et al. (2017) and Chevis et al. (2021).

The Nd isotopic compositions of the reacted seawater from the batch reaction experiment were determined on a Nu Instruments multi-collector ICP-MS at the University of Florida. The Nd isotopic composition is expressed as epsilon neodymium units, εNd (Jacobsen and Wasserburg, 1980). Before quantifying the εNd values at the University of Florida, sample preparation, matrix isolation, and pre-concentration were performed at Tulane University. The sample preparation procedure involved the use of Sep-Pak C_{18} cartridges preloaded with 300 mg of a complexing agent, which is a mixture of 65 % bis(2-ethylhexyl) hydrogen phosphate (HDEHP) and 35 % 2-ethylhexyldihydrogen phosphate (H_2MEHP), for matrix separation and pre-concentration of REEs (Shabani et al., 1992). The Sep-Pak C_{18} cartridges were pre-cleaned by filling the cartridges with 0.5 M HCl (Optima™ grade) for 24 h, followed

Table 1
Measured dissolved REE concentrations and Nd isotopic composition of the Gulf of Mexico seawater that evolved during reaction with Mississippi River sediments over 270 days of the closed-system batch reaction experiment.

		Duration (days)								
	Initial seawater	1	2	3	6	14	33	60	120	270
	Concentration (pmol kg^{-1})									
La	29.4 ± 2.1	686 ± 15	614 ± 7	994 ± 14	1420 ± 144	1302 ± 10	1606 ± 45	1036 ± 27	449 ± 13	964 ± 55
Ce	20.5 ± 2.1	834 ± 7	786 ± 11	1406 ± 18	2115 ± 66	1832 ± 39	2323 ± 99	1539 ± 12	619 ± 9	1280 ± 68
Pr	4.5 ± 1.7	104 ± 3	99 ± 3	153 ± 4	242 ± 3	193 ± 3	253 ± 9	171 ± 7	75 ± 3	144 ± 14
Nd	22.3 ± 4	497 ± 9	464 ± 17	763 ± 10	1179 ± 52	926 ± 14	1224 ± 41	789 ± 43	340 ± 5	641 ± 43
Sm	6.6 ± 3.8	119 ± 18	98 ± 4	128 ± 33	214 ± 6	181 ± 7	246 ± 39	169 ± 11	60 ± 8	130 ± 15
Eu	1.4 ± 1.9	34 ± 10	26 ± 2	36 ± 2	52 ± 4	44 ± 9	63 ± 9	32 ± 9	19 ± 4	31 ± 5
Gd	6.8 ± 1.7	168 ± 6	151 ± 8	245 ± 4	378 ± 18	289 ± 15	410 ± 12	266 ± 8	116 ± 4	191 ± 14
Tb	1.4 ± 1.8	22 ± 4	16 ± 2	24 ± 2	38 ± 4	35 ± 5	44 ± 2	32 ± 8	16 ± 2	22 ± 4
Dy	8.4 ± 1.8	126 ± 6	108 ± 4	164 ± 2	255 ± 8	198 ± 6	285 ± 12	197 ± 8	99 ± 2	128 ± 10
Ho	1.8 ± 3.5	28 ± 4	25 ± 4	35 ± 4	48 ± 4	41 ± 2	62 ± 4	43 ± 4	24 ± 2	30 ± 4
Er	4.9 ± 1.7	92 ± 4	76 ± 4	110 ± 2	168 ± 11	130 ± 4	183 ± 4	127 ± 4	70 ± 2	80 ± 4
Tm	0.8 ± 0.5	13 ± 2	11 ± 2	15 ± 2	23 ± 2	18 ± 2	24 ± 2	17 ± 2	10 ± 2	11 ± 2
Yb	4.6 ± 1.7	80 ± 2	68 ± 2	94 ± 2	145 ± 9	109 ± 4	147 ± 2	105 ± 4	59 ± 2	62 ± 6
Lu	0.7 ± 0.5	12 ± 2	11 ± 2	13 ± 2	24 ± 2	19 ± 2	24 ± 2	17 ± 2	11 ± 2	13 ± 4
HREE/LREE	3.12	2.36	2.19	1.8	1.95	1.82	1.88	2.03	2.76	1.54
Ce/Ce*	0.4	0.7	0.72	0.81	0.82	0.82	0.82	0.83	0.77	0.77
Eu/Eu*	0.89	1.29	1.26	1.25	1.08	1.11	1.16	0.84	1.2	1.1
Gd/Gd*	0.93	1.37	1.68	1.89	1.53	1.78	1.67	1.53	1.42	1.53
εNd	−9.81 ± 0.36			−9.86 ± 0.29	−9.79 ± 0.24	−9.98 ± 0.3	−9.65 ± 0.23	−10.23 ± 0.21	−9.98 ± 0.63	−9.82 ± 0.44
pH	8.1	7.6	7.4	7	6.8	6.8	6.8	7.2	7.7	7.6
Si (μmol/kg)	19.97	31.62	79.89	96.54	166.44	176.43	71.57	158.12	104.86	129.83

HREE/LREE is defined as $(Tm_N + Yb_N + Lu_N) / (La_N + Pr_N + Nd_N)$.
Anomalies: $Ce/Ce^* = 2[Ce]_N/([La]_N + [Pr]_N)$; $Eu/Eu^* = 2[Eu]_N/(0.67[Sm]_N + 0.33[Tb]_N)$; $Gd/Gd^* = [Gd]_N/(0.33[Sm]_N + 0.67[Tb]_N)$.
where $_N$ refers to shale-normalized values.

by repeated rinsing with Millipore-Q water, first leaving the water in the cartridges for 24 h and then rinsing until the pH of the dripping water matched that of the Millipore-Q water, before loading with the mixture of HDEHP and H_2MEHP. The pH of the reacted seawater samples collected for εNd analysis was adjusted to 3.5 using ammonium hydroxide (Optima™ grade) and each water sample was then passed through a preloaded C_{18} cartridge using a peristaltic pump, at a flow rate of 20 mL/min. Following the passage of the water sample, each cartridge was rinsed with 5 mL of 0.01 M HCl to remove any remaining matrix. Finally, 35 mL of 6 M HCl at a flow rate of 5 mL/min was used to elute the REEs from the cartridge into a pre-cleaned Teflon® beaker (Jeandel et al., 1998). The REE eluent was then evaporated to dryness and sent to the University of Florida.

At the University of Florida, the dried samples were dissolved with concentrated HNO_3, evaporated to near dryness, diluted with 1 M HNO_3, and then run through TruSpec resin to isolate REEs, followed by LnSpec resin to isolate Nd, as modified from Pin and Zalduegui (1997). Procedural blanks of 14 pg Nd, or a minimum of three orders of magnitude lower than sample abundances, were monitored. Samples of isolated Nd were diluted with 2 % HNO_3 to achieve ^{143}Nd monitor peak values of 2–5 V. All samples were analyzed using a desolvating nebulizer (DSN-100), and a time-resolved analysis (TRA) method adopted from Kamenov et al. (2008). All ratios were corrected for mass fractionation using ^{146}NdO/^{144}NdO = 0.7219. Also, JNdi-1 was run between every 4–5 samples and unknown samples were corrected using the difference between the average of the standard runs and the JNdi-1 value of 0.512115 (Tanaka et al., 2000). The reported εNd uncertainty is the combined 2σ internal and external error summed in quadrate (Table 1).

2.5. Geochemical modeling

Geochemical modeling of the seawater in this study was achieved using the React program of the Geochemist's Workbench® (Version 12.0.4; Bethke et al., 2018). We modified the Lawrence Livermore National Laboratory database of Delaney and Lundeen (1989) provided with the software (i.e., `thermo.dat`) by the addition of the 14 naturally occurring REEs and their inorganic aqueous complexes with carbonate, phosphate, hydroxyl, sulfate, chloride, and fluoride ions (see Johannesson et al., 2017 and supplementary materials for details). We were specifically interested in the saturation indices of secondary, REE-phosphate precipitates that have been previously reported as important to REE geochemistry in natural waters (Banfield and Eggleton, 1987; Byrne and Kim, 1993; Johannesson et al., 1995; Liu and Byrne, 1997; Pearce et al., 2013). The solubility product constants for $REEPO_{4(s)}$ phases determined by Liu and Byrne (1997) were included in the database to account for solubility limitations on the REEs owing to precipitation of such REE phosphate phases (Jonasson et al., 1985; Banfield and Eggleton, 1987; Byrne and Kim, 1993). Major ion concentrations for seawater from Pilson (2013) were used in the modeling, along with phosphate concentrations for the Gulf of Mexico for a depth of 400 m published by Shiller and Joung (2012). The REE and dissolved Si concentrations, as well as pH values measured on solution from each batch reactor were then employed in the modeling to investigate changes in REE speciation and secondary REE phosphate phase saturation states in each discrete batch reactor. Details on the modeling, example scripts, and sensitivity test results are provided in the supplementary materials.

3. Results

3.1. Characterization of the sediment particulate phases

A comparison of the surface morphology of the Mississippi River sediments before and after the batch reaction experiment is presented in Fig. 1. The SEM images of the river sediments show a change in surface texture from rough to a relatively smoother surface. Specifically, the SEM images are consistent with the removal of surface coatings on the sediment grains during reaction with seawater. The XRD result shows only trace amounts of clay materials on the surface of the sediment grains both before and

after the batch reaction experiment, and there is no substantial change in the fraction of quartz, which dominates these Mississippi River sediments. Moreover, the before and after reaction XRD results also indicate an increase of about 10 % in the relative amount of the aluminosilicate mineral, microcline (Fig. S1).

3.2. Seawater pH and dissolved silica concentrations

Again, changes in pH and dissolved Si concentrations served as monitors of the evolution of the seawater chemistry and lithogenic mineral dissolution throughout the batch reaction experiments. The pH of the reacted seawater decreased from the initial value of 8.1 to a minimum of 6.8 within the first 6 days of the experiment, before increasing to 7.9 and then 7.6 at the end of the experiment (Fig. 3a). Conversely, the dissolved Si concentration increased from an initial concentration of 19.9 μmol kg^{-1} at the start of the experiment to a peak value of 176 μmol kg^{-1} within the first 13 days of the experiment, before decreasing to 105 μmol kg^{-1} and increasing again to 130 μmol kg^{-1} at the end of the experiment. These changes in the pH and Si concentrations throughout the experiment suggest a transfer of materials from the sediments to the seawater solution followed by precipitation of secondary mineral phases through a process such as reverse weathering (e.g., Isson and Planavsky, 2018; Abbott et al., 2019).

3.3. REE concentrations and shale-normalized patterns

The dissolved REE concentrations of the reacted seawater and the "exchangeable" fraction of the Mississippi River sediments are presented in Tables 2 and S1, respectively. The "exchangeable" fraction is operationally defined as a reservoir of trace elements that are readily mobilized by changes in ionic strength due to their weak association with clays, hydrated Fe/Mn oxides surfaces, and humic substances (Tessier et al., 1979). All the REEs follow a similar trend throughout the experiment that can be characterized by an initial increase in concentrations until the concentration maxima attained after 33 days of the experiment, before decreasing to values similar to the initial concentrations at around 120 days (Fig. 4). The REE concentrations subsequently increase slightly between day 120 and the end of the experiment at 270 days (Fig. 4). For example, the Nd concentration increased by more than 50-fold from 22.3 pmol kg^{-1} in the initial seawater to 1224 pmol kg^{-1} within the first 33 days of the experiment, before decreasing by approximately a factor of 2, reaching 641 pmol kg^{-1} at the end of the experiment (Table 1; Fig. 4).

The Post-Archean Australian Shale (PAAS; Taylor and McLennan, 1985; McLennan, 1989) normalized REE patterns of the initial seawater and reacted seawater samples from the experiment are shown in Fig. 4d. The initial seawater sample exhibits an HREE enriched PAAS-normalized pattern, along with a negative cerium anomaly that is typical of seawater (e.g., Elderfield and Greaves, 1982; Elderfield, 1988; Byrne and Sholkovitz, 1996). A comparison of the normalized patterns as the experiment progressed showed little change in the overall patterns (Fig. 4d and S2). Nonetheless, the negative Ce anomalies decreased over the course of the experiments and a distinct positive gadolinium anomaly emerged. The evolution of the reacted seawater Ce and Gd anomalies throughout the experiment is also shown in Fig. 3b. Specifically, the initial seawater PAAS-normalized REE pattern exhibits a negative Ce anomaly of 0.4, which increases to 0.81 within the first 3 days of the experiment and then decreases slightly to 0.77 by the end of the experiment (Table 1). Likewise, the initial seawater Gd anomaly of 0.94 increases to 1.9 within the first 3 days of the experiment, and subsequently decreases to 1.54 by the end of the experiment (Fig. 3b).

3.4. Nd isotopic composition

The evolution of the Nd isotopic composition (i.e., εNd) of the reacted seawater is reported in Table 1 and Fig. 3c. The results

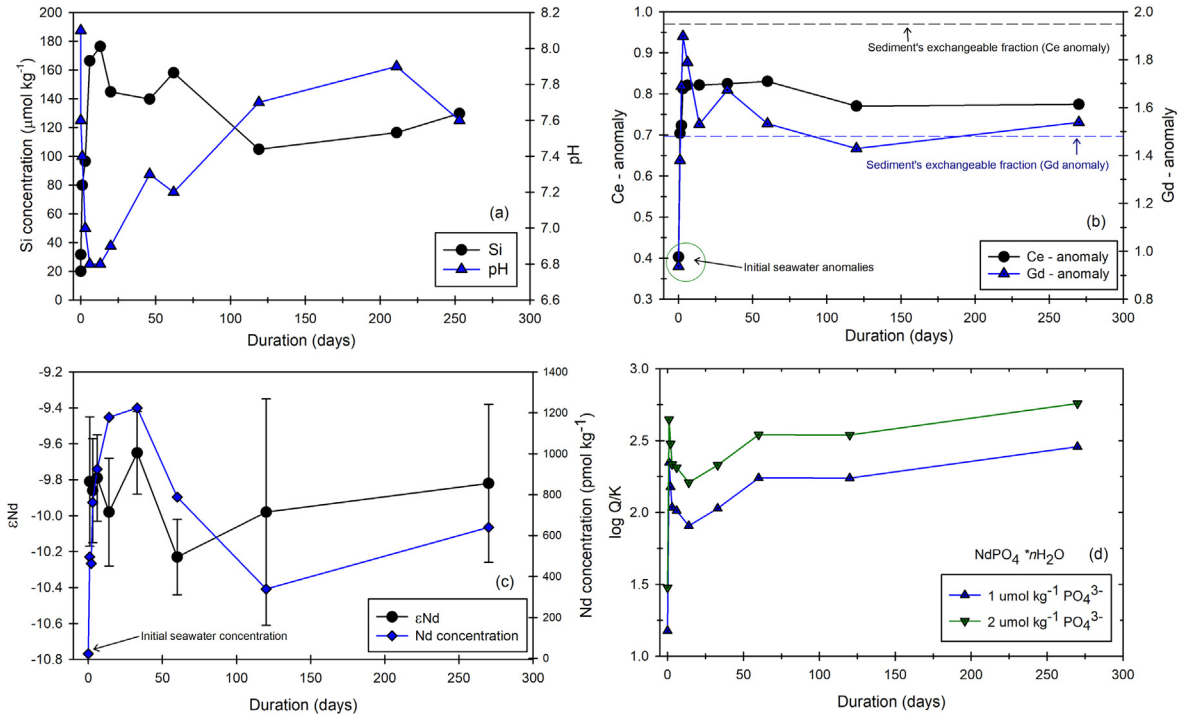

Fig. 3. Evolution of the Gulf of Mexico seawater during interaction with the Mississippi River sediments in the closed-system batch reaction experiment. Panel (a) shows pH and silica concentrations, panel (b) shows cerium (Ce) and gadolinium (Gd) anomalies, panel (c) shows neodymium isotopic composition and Nd concentration of the Gulf of Mexico seawater, panel (d) shows saturation indexes of Nd-phosphate precipitate estimated using the React program of the Geochemist's Workbench®, assuming constant seawater PO_4^{3-} at 1 and 2 μmol kg^{-1}, constant major ion concentrations, and the varying Nd, Si, and pH values measured in our batch experiment.

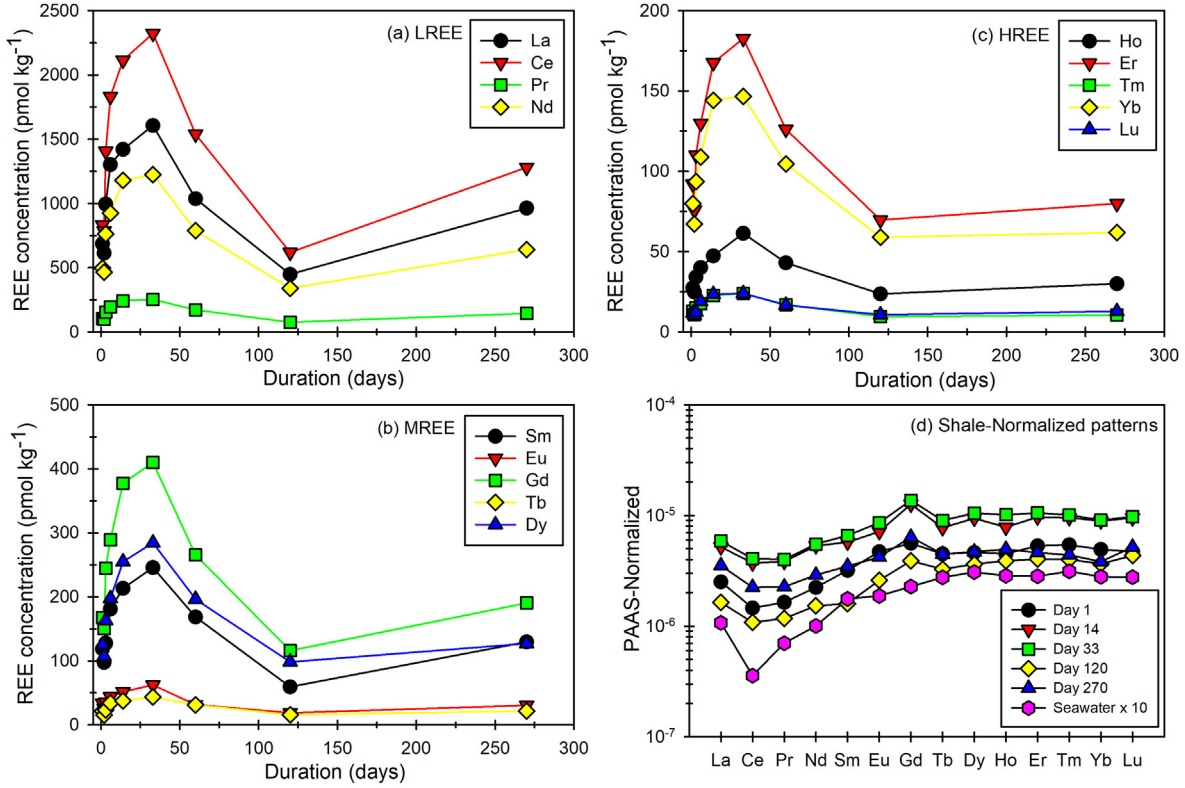

Fig. 4. Evolution of dissolved REE concentrations in the Gulf of Mexico seawater during interactions with the Mississippi River sediments throughout the closed-system batch reaction experiment. Panels (a), (b), and (c) show the concentrations of the light, middle and heavy REEs respectively and panel (d) shows the PAAS-Normalized REE patterns of the initial seawater and the reacted seawater for selected periods (Days 1, 2, 14, 33, 120, and 270).

show that changes in the εNd of the reacted seawater during the first 33 days of the experiment were<2 standard deviations (std). The first 33 days of the experiment recorded similar εNd values, with mean ± std εNd of –9.8 ± 0.12. The largest change in the isotopic composition of the reacted seawater was recorded 60 days into the experiment when εNd of –10.23 ± 0.21 was observed. The εNd values measured in the reacted seawater over the remaining period of the experiment are like values recorded during the first 33 days, with mean ± std εNd of –9.9 ± 0.11. The εNd of the reacted seawater over the entire duration of the batch reaction experiment has a mean ± std of –9.9 ± 0.2, and a range of 0.6, with the most radiogenic εNd value of –9.65 recorded on day 33 and the least radiogenic εNd value of –10.23 recorded on day 60. The most radiogenic εNd value also aligns with the Nd concentration maximum on day 33 of the experiment as shown in Fig. 3c.

4. Discussion

4.1. Evolution of the dissolved REE concentrations

Temporal changes in the dissolved Si and REE concentrations observed in this study provide clear evidence of a contribution of dissolved REEs to seawater from the dissolution of silicate phases within the Mississippi River sediments. The evolution of REE concentrations in the batch reactor experiments using the GOM seawater can be interpreted in terms of the two-way elemental transfer processes constituting "boundary exchange", which involves sediment dissolution and secondary mineral precipitation as previously described (e.g., Oelkers et al., 2011; Jones et al., 2012a, 2012b; Pearce et al., 2013; Wilson et al., 2013). The initial increase in the dissolved REE concentrations observed over the first 33 days of the experiment for each of the REEs is attributed to the dissolution of labile phases within the Mississippi River sediments. The increase in REE concentrations is consistent with reports of the benthic flux of REEs from deep-sea sediments into the overlying ocean, which has been shown to affect open ocean REE concentrations (e.g., Haley et al., 2017; Du et al., 2020; Abbott et al., 2015a, b; Abbott, 2019; Abbott et al., 2022). For example, Abbott, (2019) reported water column Nd concentrations ranging from 0 to 50 pM that reflect, in part, the impact of a benthic flux of pore water Nd with concentrations ranging from 28 to 350 pM.

The operationally defined "exchangeable" fraction of the Mississippi River sediments plays an important role during the initial dissolution of these lithogenic sediments. The "exchangeable" fraction of the Mississippi River sediments contains the lowest REE contents of all the operationally defined sequential leach fractions (Adebayo et al., 2018). Nevertheless, it still maintains REE contents that are several orders of magnitude greater than the REE concentrations in typical seawater. Specifically, a Nd content of 326 nmol kg^{-1} was reported in the "exchangeable" fraction of the Mississippi River sediments (Adebayo et al., 2018), whereas the Nd concentration of the initial GOM seawater used in our experiments was 22.3 pmol kg^{-1} (Tables 1 and S1). Therefore, the concentration difference between the "exchangeable" fraction of the sediments and seawater in this study strongly favors the mobilization of REEs into the reacted seawater.

Secondary mineral precipitation appears to be another important process influencing the evolution of REE concentrations in the batch reactors containing Mississippi River sediments and open GOM seawater, as observed via the decrease in dissolved REE concentrations beyond 33 days. Potential secondary minerals that could scavenge the dissolved REEs in this experiment include Fe/Mn oxides/oxyhydroxides produced by oxidation of Fe^{2+}-bearing minerals that could precipitate in the reacted seawater

and/or secondary REE-phosphate co-precipitates that are reportedly super-saturated in seawater (Byrne and Kim, 1993; Oelkers et al., 2008; Roncal-Herrero et al., 2011; Pearce et al., 2013). Several studies have also demonstrated the importance of clay minerals to the cycling of REEs in the ocean, suggesting that these clays serve as important sources and sinks of REEs (e.g., Cullers et al., 1975; Haley et al., 2017; Abbott, 2019; Paul et al., 2019; Du et al., 2020; Abbott et al., 2022). Moreover, clay minerals may also play a major role in controlling benthic REE fluxes to the overlying seawater (Abbott et al., 2019).

In addition to scavenging by Fe/Mn oxides/oxyhydroxides, precipitation of secondary REE phosphate minerals, and adsorption onto clay minerals (e.g., Jonasson et al., 1985; Goldstein and Jacobsen, 1988; Byrne and Kim, 1993; Johannesson et al., 1995; Sholkovitz, 1995; Sholkovitz and Szymczak, 2000; Adebayo et al., 2018), it is also possible that "reverse weathering" reactions, whereby the products of the weathering of aluminosilicate minerals take up cations and silica forming cation-enriched aluminosilicates, are occurring during the batch reaction experiment in this study. The formation of cation-enriched aluminosilicate minerals has been reported as potentially important in controlling the chemistry of the ocean, and has been characterized by an increase in secondary, potassium-rich silicate minerals (e.g., Mackenzie and Kump, 1995; Michalopoulos and Aller, 1995; Isson and Planavsky, 2018). The reported increase in the relative amount of K-aluminosilicate minerals (i.e., microcline) within the Mississippi River sediments over the course of the batch reaction experiments may indicate that reverse weathering processes occurred in our experiments. Abbott et al. (2019) also reported authigenic clay formation or "reverse weathering" as exerting important controls on REE cycling in the ocean, specifically the balance between detrital dissolution and authigenic uptake.

The evolution of dissolved REE concentrations in this study closely resembles the trends reported for the evolution of seawater strontium and alkali earth metal concentrations during reaction with basaltic riverine sediments from the Hvítá River and the Borgarfjörður estuary in western Iceland (Jones et al., 2012a). However, a similar study that investigated the evolution of REE concentrations in seawater during reaction with basaltic particulate materials reported that the Nd concentration decreased throughout their experiment (Pearce et al., 2013). These researchers attributed this decrease to the precipitation of the REE-phosphate mineral, rhabdophane, based on PHREEQC calculations and experimental data (Pearce et al., 2013).

The evolution of the seawater dissolved REE concentrations during reaction with the Mississippi River sediments in this study (Fig. 4) also appears to capture both the initial dissolution, desorption, and/or remineralization of the lithogenic river sediments as well as the precipitation of secondary minerals containing REEs and/or adsorption that are generally thought to characterize the boundary exchange process (Lacan and Jeandel, 2005; Arsouze et al., 2009; Jeandel et al., 2011; Jeandel, 2016). Experimental data and numerical simulations demonstrate that the REE-phosphate mineral, rhabdophane, is super-saturated in seawater (Oelkers et al., 2008; Roncal-Herrero et al., 2011; Pearce et al., 2013), making it a potential sink for the REEs in our closed-system batch reaction experiment. Moreover, seawater is saturated relative to LREE-phosphate co-precipitates, which suggests that these secondary minerals limit the solubility of REEs in the ocean (e.g., Jonasson et al., 1985; Byrne and Kim, 1993). Geochemical modeling (Fig. 3d) predicts that LREE-phosphate precipitates are oversaturated of the REEs in the batch solutions throughout our experiment. Therefore, our results and those of Pearce et al. (2013) are consistent with previous studies that suggest that REE-phosphates are important in controlling REE concentrations and may also be important in limiting REE concentrations in seawater and other natural waters (Jonasson et al., 1985; Byrne and Kim, 1993; Johannesson et al., 1995).

Overall, the REE concentrations in the reacted seawater at the end of the experiment (270 days) were 13 to 62-fold greater than those of the initial seawater. We attribute these observations to the dissolution of lithogenic sediments followed by REE uptake by secondary minerals such as REE-phosphate co-precipitates and/or adsorption (Fig. 5a). Our experiments indicate that the net release of REEs during the dissolution of lithogenic sediments exceeded the amount of REEs taken up by secondary mineral precipitation. Specifically, the LREEs exhibit the greatest increase in concentration at the end of the experiment, with Nd showing a 28-fold increase in concentration, whereas the HREEs exhibit the least increase as shown by Yb, which increased by a factor of 13 (Fig. 5a).

The Pearson correlation coefficients (r) and the relationship between the REEs and Si concentrations in the reacted seawater (Fig. 5b) suggest that silicate minerals, which are the bulk of the river sediments, are dissolving and releasing H_4SiO_4 along with REEs. Specifically, the correlation coefficients between LREE and Si concentrations in the reacted seawater in this experiment ranged from 0.61 to 0.64, with a mean ± std of 0.62 ± 0.01; $p < 0.05$ (two-tailed student *t*-test with $\alpha = 0.05$), correlation coefficients

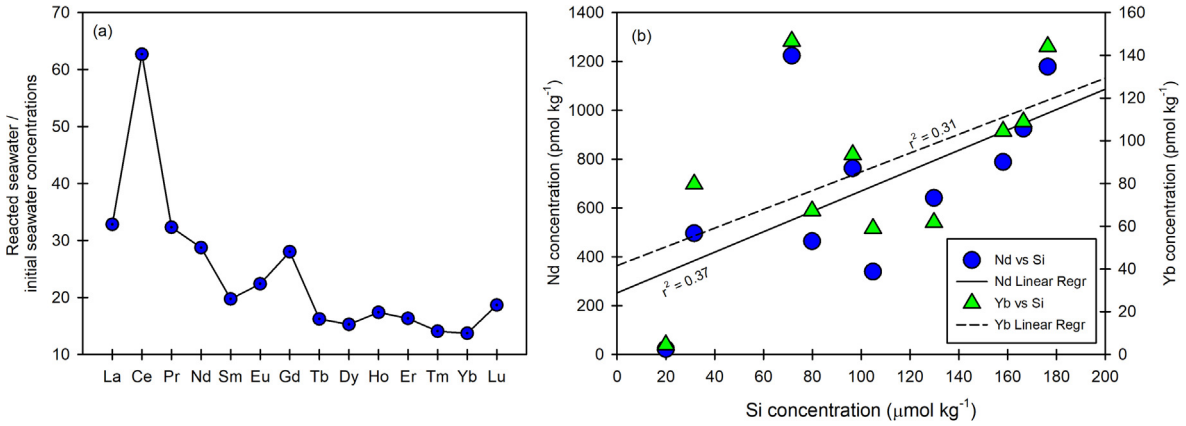

Fig. 5. The ratio of dissolved REE concentrations in the reacted seawater on Day 270 to initial seawater concentrations (Panel a). Panel (b) shows the relationship between select REEs (Nd and Yb) and Si concentrations throughout the closed system batch reaction experiment involving Gulf of Mexico seawater and the Mississippi River sediments, where the Pearson correlation coefficient (r) between Nd and Si is 0.61, $p < 0.05$ and r for Yb and Si is 0.56, $p < 0.05$.

for the MREE and Si concentrations range from 0.44 to 0.59, with a mean ± std of 0.55 ± 0.06; $p < 0.05$, and correlation coefficients for the HREE and Si concentrations range from 0.54 to 0.64, with a mean ± std of 0.57 ± 0.04; $p < 0.05$. Also, the slight increase in REE concentrations between days 120 and 270 suggests possible remobilization of REEs into the solution, although a longer-term experiment would be necessary to better understand this observation.

4.2. Evolution of the dissolved REE fractionation patterns

The PAAS-normalized REE patterns throughout this experiment also capture the two-way elemental transfer involving dissolution of lithogenic sediments and secondary mineral precipitation in the system (Fig. 4d). A shift from the HREE enriched pattern in the initial seawater (shale normalized HREE/LREE of 3.12, Table 1) to a less HREE enriched pattern as the reaction progressed (HREE/LREE of 1.88 on day 33, peak REE concentrations) is attributed to the greater abundance of the LREEs than the MREEs and HREEs in the silicate minerals being dissolved. As noted above, the correlation between REE and Si concentrations in the reacted seawater suggests that the dissolution of silicate minerals is the primary source of the REEs flux into the dissolved phase during the experiment. It is well known that common rock-forming silicate minerals (except for a few minerals such as zircon and garnet, which are highly resistant to weathering) contain markedly lower amounts of MREEs and HREEs relative to the LREEs (e.g., a factor of 3 to 5 lower HREE contents, Gromet and Silver, 1983; McLennan and Taylor, 2012). Also, the mean of HREE concentrations in the operationally defined "exchangeable" fraction of the Mississippi River sediments used in this study (Table S1) is a factor of 2 lower than the mean of the LREE contents (Adebayo et al., 2018). The greater abundance of the LREEs in the labile mineral phases of the reacting sediments explains the shift in the PAAS-normalized pattern of the seawater from HREE enriched to a less fractionated pattern during the batch reactor experiment.

A comparison of the Ce and Gd anomalies in the initial seawater to anomalies in the "exchangeable" fraction of the sediments used in this experiment also highlights the influence of dissolution of labile phases within the sediments on the dissolved REE concentrations in the reacted seawater. Specifically, the Ce anomaly evolved from 0.4 in the initial seawater to a mean ± std of 0.79 ± 0.05 in the reacted seawater over the entire duration of the experiment, which is closer to the Ce anomaly of 0.98 reported in the "exchangeable" fraction of the sediments (Tables 1 and S1). The decrease in negative Ce anomaly of the reacted seawater possibly reflects the release of Ce that is preferentially removed from river water relative to its neighboring REEs due to tetravalent Ce removal (Sholkovitz, 1995; Shiller, 2002; Adebayo et al., 2018). Similarly, the Gd anomaly evolved from 0.94 in the initial seawater to a mean ± std of 1.61 ± 0.17 in the reacted seawater over the entire duration of the experiment. The Gd anomaly of the reacted seawater is likewise closer to the Gd anomaly of 1.48 reported in the "exchangeable" fraction of the sediments. Although several studies have reported the significant impact of anthropogenic Gd on the dissolved Gd concentrations in river waters impacted by municipal wastewater, Gd anomalies observed in this study are within the range reported in unpolluted waters and less than values (i.e., ≥ 4) reported for waters impacted by anthropogenic inputs (e.g., Kim et al., 1991; Bau and Dulski, 1996; Adebayo et al., 2018).

4.3. Evolution of the dissolved Nd isotopic composition

Unlike the study by Pearce et al. (2013), the Nd isotopic composition of GOM seawater reacted with Mississippi River sediments did not change substantially throughout our batch reaction experiment (Fig. 3c). Indeed, the εNd values of the reacted seawater varied by<0.58 εNd units and thus remained within the range of analytical uncertainty throughout the 270-day experiment (Table 1; Fig. 3c). The nearly constant εNd values are opposite of what "boundary exchange" classically predicts and reflect the fact that the εNd of labile mineral phases within the Mississippi River sediments are essentially the same as the εNd of the initial GOM seawater employed in the experiment. This observation is consistent with model and experimental reports that isotopic compositions of the reacting components of a system must be unique to drive a significant change in isotopic composition (e.g., Jones et al., 2012a; Pearce et al., 2013; Wilson et al., 2013; Abbott *et al.*, 2015; Jeandel and Oelkers, 2015; Haley et al., 2017; Abbott et al., 2022).

More specifically, the εNd values measured in the acid leachable fraction of suspended particulate matter (SPM) from the Mississippi River are −9.95 and −9.77 (Adebayo et al., 2018), whereas the εNd of the GOM seawater sample is −9.81 ± 0.36. We note that the εNd for our GOM seawater sample compares well with the analysis of Osborne et al. (2014) for a Gulf of Mexico sample (Station 194–13, 300 – 531 m depth, mean ± std εNd of −9.63 ± 0.45). Station 194–13 from Osborne et al. (2014) was selected for comparison because it is located within the Gulf (about 500 km from our sampling location), and samples from depths below 300 m were selected because they are closest to the collection depth of the seawater sample used in our study. Seawater samples from Osborne et al. (2014) collected from depths shallower than 300 m showed higher εNd variability. These εNd values strongly suggest that the εNd of GOM seawater reflects, at least in part, dissolution of lithogenic Mississippi River sediments. Therefore, dissolution of lithogenic Mississippi River sediments would be expected to contributes a benthic εNd flux with a composition like the labile fraction of Mississippi River sediments (e.g., Wilson et al., 2013; Abbott et al., 2019; Paul et al., 2019). Although we did not observe significant changes in εNd like similar experiments that employed basaltic material, we note that the εNd of the reacted seawater reached its most radiogenic value (-9.65) on day 33, which corresponds to the day with the highest dissolved REE concentrations.

When compared to the evolution of the Nd isotopic composition observed in the basaltic systems reported by Pearce et al. (2013), the absence of substantial changes in the εNd of the system in our study becomes more obvious (Fig. 6). The seawater sample employed by Pearce et al. (2013) has a similar εNd value (-9.57) to the GOM seawater sample used in our experiments (-9.81) prior to reactions with the sediments (Fig. 6). However, as the experiments progressed, the systems studied by Pearce et al. (2013) experienced ≥ 3 εNd change within 7 days as their εNd tended toward more radiogenic values reflecting the εNd of the reacting radiogenic basaltic sediments.

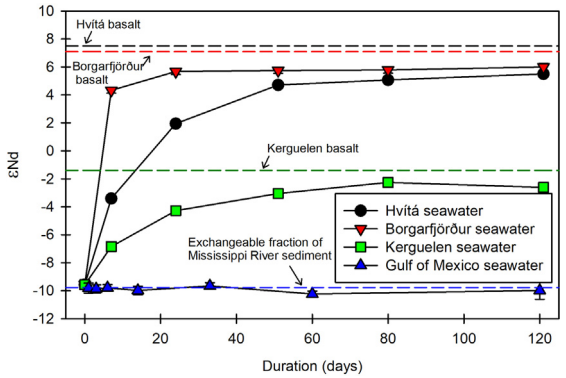

Fig. 6. A comparison of the evolution of Nd isotopic composition of the reacted seawater during the closed-system batch reaction experiment between seawater and sediments in this study (Gulf of Mexico seawater) to values reported in a previous study that used basaltic particulate materials (Pearce et al., 2013).

Specifically, the εNd of the basaltic Hvítá sand is 7.50; the basaltic Borgarfjörður sand εNd is 7.17; and the Kerguelen basalt has an εNd of −1.4 (Pearce et al., 2013). In contrast, we measured εNd of −9.95 and −9.77 for the acid leachable fraction of the Mississippi River SPM, representative of εNd of the riverbank sediments studied by Adebayo et al. (2018). It is clear from this comparison that εNd values of the Mississippi River sediments and the GOM seawater are not sufficiently distinct to drive a substantial change in the εNd of the reacted seawater in this study. Instead, the Mississippi River sediments may essentially buffer the εNd composition of GOM seawater by the dissolution of the labile fraction of these lithogenic sediments. In other words, the εNd composition of GOM seawater appears to be controlled by dissolution of lithogenic sediments delivered to the basin by the Mississippi River.

4.4. Implications for ocean margin processes

In discussing the implications of our study, we acknowledge that closed-system laboratory experiments like this study are unable to capture all the complex processes occurring in estuaries or on the continental shelf/slope, but they offer an important window into these processes that control ocean geochemistry. The results of our experiment are consistent with the release of REEs from lithogenic sediments of continental origins (i.e., silicic) by the dissolution of the more labile fractions of these sediments. By comparing the Nd concentration maximum during our experiment (1.22 nmol kg^{-1}, day 33, Table 1, Fig. 4) to the Nd concentration (326 nmol kg^{-1}) measured in the "exchangeable" fraction of the Mississippi River sediment (Adebayo et al., 2018), we estimate that although only about 0.37 % of the available Nd in the "exchangeable" fraction is mobilized, this limited mobilization can still substantially alter the Nd concentration of seawater.

Despite the differences in reactivity between basaltic and silicic sediments, our estimated 0.37 % mobilization agrees surprisingly well with the findings by Pearce et al. (2013), who estimated a release of 0.38 % of Nd from basaltic estuarine sediments and release of 0.25 % of Nd from river sediments of similar basaltic composition. The similarity in Nd mobilization between our data and the study by Pearce et al. (2013) suggests that, in terms of Nd isotopes, the more reactive components in silicic continental lithogenic material are almost as reactive as those in basaltic material. However, it took about 30 days to achieve the maximum sediments exchange of Nd in the case of silicic sediments in our study, compared to < 10 days for sediment exchange of Nd reported by Pearce et al. (2013), and 8 – 10 days suggested based on in-situ measurements by Rousseau et al. (2015). Nevertheless, Pearce et al. (2013) observed a drop in the dissolved Nd concentration during the initial reaction period. In contrast, we observed an increase in concentration (Fig. 4). Our results are consistent with the findings from studies of benthic fluxes, whereby the dissolution of silicic, lithogenic sediments along continental margins can significantly impact the dissolved REE concentrations of seawater (e.g., Wilson et al., 2013; Abbott et al., 2019; Paul et al., 2019).

Furthermore, when we normalized the dissolved REE concentrations in the reacted seawater by the REE concentrations in the initial seawater in this study, the REE concentrations of the seawater increased by an average (±1σ) factor of 24 ± 12 across the REE series by the end of the experiment (Fig. 5). The net gain of dissolved REEs observed in the reacted seawater in this study offers a possible explanation for the substantially lower removal of the REEs (e.g., about 50 % Nd removal) observed in the Mississippi River estuary (Adebayo et al., 2018), compared to the amount of REE removal observed in the Amazon estuary where up to 90 % REE removal during estuarine mixing was reported (e.g., Rousseau et al., 2015).

5. Conclusions

Results from a 270-day batch reaction experiment between Gulf of Mexico (GOM) seawater and Mississippi River sediments show evidence of substantial changes in the dissolved REE concentrations but limited to no changes in the εNd of the reacted seawater. The concentration changes include up to a 100-fold increase in dissolved REE concentrations coupled with an increase in Si concentrations and a decrease in pH within the first 33 days of the experiment, which we attribute to the dissolution of the sediment's more labile oxide and silicate mineral phases. The observed increase in REE concentrations subsequently reverses with reaction beyond 33 days followed by a slight increase again at the end of the experiment. We attribute the decrease in REE concentrations in the batch reaction experiments to the formation and uptake of REEs by secondary minerals like REE-phosphates, sorption, and possibly "reverse weathering" reactions. Evolution of the seawater Ce anomalies, Gd anomalies, and HREE/LREE ratios also confirm that REEs were released into solution and subsequently removed by secondary mineral precipitation during the experiment. Notably, less than 1 % of the REE contents of the operationally defined "exchangeable" fraction of the Mississippi River sediments was mobilized in our experiment, which nevertheless resulted in a net 13–62-fold increase in the REE concentrations of the Gulf seawater throughout the experiment.

The absence of a substantial change in the εNd composition of the reacted seawater in this study compared to previous studies is attributed to the similarity between the εNd of the reacting Mississippi River sediments and GOM seawater, relative to previous studies where the basaltic sediments involved are far more radiogenic than the seawater. However, we show that silicic lithogenic sediments may be almost as reactive as basaltic material as observed by the change in REE concentrations, and therefore a major contributor to boundary exchange and seawater εNd. These observations suggest that in addition to altering seawater in regions proximal to basaltic ocean islands, boundary exchange process may also influence seawater compositions in regions proximal to silicic sources with distinct radiogenic signature, such as the highly non-radiogenic Archean rocks surrounding the Baffin Bay in the Canadian Arctic. Finally, our experiments strongly suggest that the εNd composition of GOM seawater is controlled by the dissolution of lithogenic sediments delivered to the basin by the Mississippi River.

Data availability

Data will be made available on request.

Declaration of Competing Interest

The authors declare that they have no known competing financial interests or personal relationships that could have appeared to influence the work reported in this paper.

Acknowledgments

Segun Adebayo wishes to thank the Department of Earth and Environmental Sciences at Tulane University for support via graduate assistantships and the Volkes Fellowship. Dr. Karen Johannesson thanks Michael and Mathilda Cochran for endowing the Cochran Family Professorship at Tulane University, which helped support the sampling and geochemical analyses. Johannesson's efforts were also partially supported by NSF award OCE-1850768. Dr. Ellen Martin thanks George Kamenov for assistance in Nd isotopic analyses. We are grateful to Dr. Alex Kolker at the Louisiana

Universities Marine Consortium (LUMCON) and Dr. Vernon Asper at the University of Southern Mississippi for assistance in sampling the Gulf of Mexico seawater, Tanya Goehring for assistance with XRD analysis, Dr. He Jibao for assistance with the SEM-EDS characterization, and Dr. Deborah Grimm for assistance with the ICP-MS analysis. Finally, we thank the associate editor, Dr. Noah Planavsky for his expert handling of our manuscript, as well as very helpful reviews by Dr. Brian Haley and two anonymous reviewers, all of which improved this contribution.

Appendix A. Supplementary material

Supplementary material to this article can be found online at https://doi.org/10.1016/j.gca.2022.08.024.

References

Abbott, A.N., 2019. A benthic flux from calcareous sediments results in non-conservative neodymium behavior during lateral transport: A study from the Tasman Sea. Geology 47 (4), 363–366.
Abbott, A.N., Haley, B.A., McManus, J., Reimers, C.E., 2015a. The sedimentary flux of dissolved rare earth elements to the ocean. Geochim. Cosmochim. Acta 154, 186–200.
Abbott, A.N., Haley, B.A., McManus, J., 2015b. Bottoms up: Sedimentary control of the deep North Pacific Ocean's ε_{Nd} signature. Geology 43, 1035–1038.
Abbott, A.N., Löhr, S., Trethewy, M., 2019. Are clay minerals the primary control on the oceanic rare earth element budget? Front. Mar. Sci. 504.
Abbott, A.N., Löhr, S.C., Payne, A., Kumar, H., Du, J., 2022. Widespread lithogenic control of marine authigenic neodymium isotope records? Implications for paleoceanographic reconstructions. Geochim. Cosmochim. Acta 319, 318–336.
Adebayo, S.B., Cui, M., Hong, T., Johannesson, K.H., Martin, E.E., 2018. Rare earth elements geochemistry and Nd isotopes in the Mississippi River and the Gulf of Mexico mixing zone. Front. Mar. Sci. 5, 166.
Adebayo, S.B., Cui, M., Hong, T., Akintomide, O., Kelly, R.P., Johannesson, K.H., 2020. Rare earth element cycling and reaction path modeling across the chemocline of the Pettaquamscutt River estuary, Rhode Island. *Geochim. Cosmochim. Acta* 284, 21–42.
Akintomide, O.A., Adebayo, S., Horn, J.D., Kelly, R.P., Johannesson, K.H., 2021. Geochemistry of the redox-sensitive trace elements molybdenum, tungsten, and rhenium in the euxinic porewaters and bottom sediments of the Pettaquamscutt River estuary, Rhode Island. *Chem. Geol.* 584, 120499.
Arsouze, T., Dutay, J.C., Lacan, F., Jeandel, C., 2009. Reconstructing the Nd oceanic cycle using a coupled dynamical-biogeochemical model. Biogeosciences 6, 1–18.
Banfield, J.E., Eggleton, R.A., 1987. Apatite replacement and rare earth mobilization, fractionation, and fixation during weathering. Clays Clay Miner. 37, 113–127.
Bau, M., Dulski, P., 1996. Anthropogenic origin of positive gadolinium anomalies in river waters. Earth Planet. Sci. Lett. 143 (1–4), 245–255.
Bethke, C.M., Farrell, B., Yeakel, S., 2018. The Geochemist's Workbench", Release 9.0. *GWB Essentials Guide. Aqueous Solutions*, LLC, Champaign, IL. **141**.
Blaser, P., Gutjahr, M., Pöppelmeier, F., Frank, M., Kaboth-Bahr, S., Lippold, J., 2020. Labrador Sea bottom water provenance and REE exchange during the past 35,000 years. Earth Planet. Sci. Lett. 542, 116299.
Boyd, P.W., Ellwood, M.J., 2010. The biogeochemical cycle of iron in the ocean. Nat. Geosci. 3 (10), 675–682.
Byrne, R.H., Kim, K.H., 1993. Rare earth precipitation and coprecipitation behavior: the limiting role of PO43− on dissolved rare earth concentrations in seawater. Geochim. Cosmochim. Acta 57 (3), 519–526.
Byrne, R.H., Sholkovitz, E.R., 1996. Marine chemistry and geochemistry of the lanthanides. Handbook Phys. Chem. Rare Earths 23, 497–593.
Chester, R., Murphy, K.J.T., Lin, F.J., Berry, A.S., Bradshaw, G.A., Corcoran, P.A., 1993. Factors controlling the solubilities of trace metals from non-remote aerosols deposited to the sea surface by the 'dry'deposition mode. Mar. Chem. 42 (2), 107–126.
Chevis, D.A., Johannesson, K.H., Burdige, D.J., Cable, J.E., Martin, J.B., Roy, M., 2015. Rare earth element cycling in a sandy subterranean estuary in Florida, USA. Mar. Chem. 176, 34–50.
Chevis, D.A., Mohajerin, T.J., Yang, N., Cable, J.E., Rasbury, E.T., Hemming, S.R., Burdige, D.J., Martin, J.B., White, C.D., Johannesson, K.H., 2021. Neodymium isotope geochemistry of a subterranean estuary. Front. Water 3, 778344.
Cullers, R.L., Chaudhuri, S., Arnold, B., Lee, M., Wolf Jr, C.W., 1975. Rare earth distributions in clay minerals and in the clay-sized fraction of the Lower Permian Havensville and Eskridge shales of Kansas and Oklahoma. Geochim. Cosmochim. Acta 39 (12), 1691–1703.
Delaney, J.M., Lundeen, S.R., 1989. The LNLL thermochemical database. *Lawrence Livermore National Laboratory, Report* UCRL-21658.
Du, J., Haley, B.A., Mix, A.C., 2020. Evolution of the Global Overturning Circulation since the Last Glacial Maximum based on marine authigenic neodymium isotopes. Quat. Sci. Rev. 241, 106396.
Dupré, B., Dessert, C., Oliva, P., Goddéris, Y., Viers, J., François, L., Millot, R., Gaillardet, J., 2003. Rivers, chemical weathering and Earth's climate. C.R. Geosci. 335 (16), 1141–1160.
Elderfield, H., 1988. The oceanic chemistry of the rare-earth elements. Philos. Trans. R. Soc. Lond.n Ser. A, Math. Phys. Sci. 325 (1583), 105–126.
Elderfield, H., Greaves, M.J., 1982. The rare earth elements in seawater. Nature 296 (5854), 214.
Gaillardet, J., Dupré, B., Allègre, C.J., 1999. Geochemistry of large river suspended sediments: silicate weathering or recycling tracer? Geochim. Cosmochim. Acta 63 (23–24), 4037–4051.
Gaillardet, J., Viers, J., Dupré, B., 2003. Trace elements in river waters. Treat. Geochem. 5, 605.
Georg, R.B., Reynolds, B.C., Frank, M., Halliday, A.N., 2006. New sample preparation techniques for the determination of Si isotopic compositions using MC-ICPMS. Chem. Geol. 235 (1–2), 95–104.
Gíslason, S.R., Oelkers, E.H., 2003. Mechanism, rates, and consequences of basaltic glass dissolution: II. An experimental study of the dissolution rates of basaltic glass as a function of pH and temperature. Geochim. Cosmochim. Acta 67, 3817–3832.
Goldstein, S.J., Jacobsen, S.B., 1988. Rare earth elements in river waters. Earth Planet. Science Lett. 89 (1), 35–47.
Greaves, M.J., Elderfield, H., Klinkhammer, G.P., 1989. Determination of the rare earth elements in natural waters by isotope-dilution mass spectrometry. Anal. Chim. Acta 218, 265–280.
Greaves, M.J., Statham, P.J., Elderfield, H., 1994. Rare earth element mobilization from marine atmospheric dust into seawater. Mar. Chem. 46 (3), 255–260.
Gromet, L.P., Silver, L.T., 1983. Rare earth element distributions among minerals in a granodiorite and their petrogenetic implications. Geochim. Cosmochim. Acta 47 (5), 925–939.
Gudbrandsson, S., Wolff-Boenisch, D., Gislason, S.R., Oelkers, E.H., 2011. An experimental study of crystalline basalt dissolutions from $2 \leq$ pH ≤ 11 and from 5 to 75°C. Geochim. Cosmochim. Acta 75, 5496–5509.
HACH, C., 2007. HACH DR 2800 Spectrophotometer Procedures manual. Edition 2. *Catalog Number DOC022.53.00725*, Hach Company, Germany.
Haley, B.A., Klinkhammer, G.P., McManus, J., 2004. Rare earth elements in pore waters of marine sediments. Geochim. Cosmochim. Acta 68 (6), 1265–1279.
Haley, B.A., Du, J., Abbott, A.N., McManus, J., 2017. The impact of benthic processes on rare earth element and neodymium isotope distributions in the oceans. Front. Mar. Sci. 4, 426.
Holeman, J.N., 1968. The sediment yield of major rivers of the world. Water Resour. Res. 4 (4), 737–747.
Howe, J.N., Piotrowski, A.M., Rennie, V.C., 2016. Abyssal origin for the early Holocene pulse of unradiogenic neodymium isotopes in Atlantic seawater. Geology 44 (10), 831–834.
Isson, T.T., Planavsky, N.J., 2018. Reverse weathering as a long-term stabilizer of marine pH and planetary climate. Nature 560 (7719), 471–475.
Jacobsen, S.B., Wasserburg, G.J., 1980. Sm-Nd isotopic evolution of chondrites. Earth Planet. Sci. Lett. 50 (1), 139–155.
Jeandel, C., 2016. Overview of the mechanisms that could explain the 'Boundary Exchange'at the land–ocean contact. Philos. Trans. R. Soc. Lond.n Ser. A, Math. Phys. Sci. 374 (2081), 20150287.
Jeandel, C., Oelkers, E.H., 2015. The influence of terrigenous particulate material dissolution on ocean chemistry and global element cycles. Chem. Geol. 395, 50–66.
Jeandel, C., Thouron, D., Fieux, M., 1998. Concentrations and isotopic compositions of neodymium in the eastern Indian Ocean and Indonesian straits. Geochim. Cosmochim. Acta 62 (15), 2597–2607.
Jeandel, C., Peucker-Ehrenbrink, B., Jones, M.T., Pearce, C.R., Oelkers, E.H., Godderis, Y., Lacan, F., Aumont, O., Arsouze, T., 2011. Ocean margins: The missing term in oceanic element budgets? Eos, Trans. Am. Geophys. Union 92 (26), 217–218.
Johannesson, K.H., Lyons, W.B., 1994. The rare earth element geochemistry of Mono Lake water and the importance of carbonate complexing. Limnol. Oceangr. 39, 1141–1154.
Johannesson, K.H., Lyons, W.B., Stetzenbach, K.J., Byrne, R.H., 1995. The solubility control of rare earth elements in natural terrestrial waters and the significance of PO 4 3− and CO 3 2− in limiting dissolved rare earth concentrations: A review of recent information. Aquat. Geochem. 1 (2), 157–173.
Johannesson, K.H., Lyons, W.B., 1995. Rare-earth element geochemistry of Colour Lake, and acididic freshwater lake lake on Axel Heiberg Island, Northwest Territories, Canada. *Chem. Geol.* 119, 209–223.
Johannesson, K.H., Stetzenbach, K.J., Hodge, V.F., Kreamer, D.K., Zhou, X., 1997. Delineation of ground-water flow systems in the southern Great Basin using aqeous rare earth element distributions. Ground Water 35, 807–819.
Johannesson, K.H., Chevis, D.A., Burdige, D.J., Cable, J.E., Martin, J.B., Roy, M., 2011. Submarine groundwater discharge is an important net source of light and middle REE to coastal waters of the Indian River Lagoon, Florida, USA. Geochim. Cosmochim. Acta 75 (3), 825–843.
Johannesson, K.H., Palmore, C.D., Fackrell, J., Prouty, N.G., Swarzenski, P.W., Chevis, D.A., Telfeyan, K., White, C.D., Burdige, D.J., 2017. Rare earth element behavior during groundwater–seawater mixing along the Kona Coast of Hawaii. Geochim. Cosmochim. Acta 198, 229–258.
Johnson, C.M., Beard, B.L., Albarede, F., 2004. Geochemistry of non-traditional stable isotopes. Rev. Mineral. Geochem. 55, 1–454.
Jonasson, R.G., Bancroft, G.M., Nesbut, H.W., 1985. Solubilities of some hydrous REE phosphates with implications for diagenesis and seawater concentrations. Geochim. Cosmochim. Acta 49, 2133–2139.

Jones, M.T., Pearce, C.R., Oelkers, E.H., 2012a. An experimental study of the interaction of basaltic riverine particulate material and seawater. Geochim. Cosmochim. Acta 77, 108–120.
Jones, M.T., Pearce, C.R., Jeandel, C., Gislason, S.R., Eiriksdottir, E.S., Mavromatis, V., Oelkers, E.H., 2012b. Riverine particulate material dissolution as a significant flux of strontium to the oceans. Earth Planet. Sci. Lett. 355, 51–59.
Kamenov, G.D., Perfit, M.R., Mueller, P.A., Jonasson, I.R., 2008. Controls on magmatism in an island arc environment: study of lavas and sub-arc xenoliths from the Tabar–Lihir–Tanga–Feni island chain, Papua New Guinea. Contrib. Miner. Petrol. 155 (5), 635–656.
Kim, K.H., Byrne, R.H., Lee, J.H., 1991. Gadolinium behavior in seawater: a molecular basis for gadolinium anomalies. Mar. Chem. 36 (1–4), 107–120.
Lacan, F., Jeandel, C., 2005. Neodymium isotopes as a new tool for quantifying exchange fluxes at the continent–ocean interface. Earth Planet. Sci. Lett. 232 (3–4), 245–257.
Lawrence, M.G., Kamber, B.S., 2006. The behaviour of the rare earth elements during estuarine mixing—revisited. Mar. Chem. 100 (1–2), 147–161.
Liu, X., Byrne, R.H., 1997. Rare earth and yttrium phosphate solubilities in aqueous solution. Geochim. Cosmochim. Acta 61 (8), 1625–1633.
Mackenzie, F.T., Kump, L.R., 1995. Reverse weathering, clay mineral formation, and oceanic element cycles. Science 270 (5236), 586.
McKee, B.A., Aller, R.C., Allison, M.A., Bianchi, T.S., Kineke, G.C., 2004. Transport and transformation of dissolved and particulate materials on continental margins influenced by major rivers: benthic boundary layer and seabed processes. Cont. Shelf Res. 24 (7–8), 899–926.
McLennan, S.M., Taylor, S.R., 2012. Geology, geochemistry, and natural abundances of the rare earth elements. In: Atwood, D.A. (Ed.), The Rare Earth Elements: Fundamentals and Applications. John Wiley and Sons, Chichester, UK, pp. 1–19.
McLennan, S.M., 1989. Rare earth elements in sedimentary rocks; influence of provenance and sedimentary processes. Rev. Mineral. Geochem. 21, 169–200.
Michalopoulos, P., Aller, R.C., 1995. Rapid clay mineral formation in Amazon delta sediments: reverse weathering and oceanic elemental cycles. Science 270 (5236), 614–617.
Navarre-Sitchler, A., Brantley, S., 2007. Basalt weathering across scales. Earth Planet. Sci. Lett. 261, 321–334.
Oelkers, E.H., Gislason, S.R., Eiriksdottir, E.S., Jones, M.T., Pearce, C.R., Jeandel, C., 2011. The role of riverine particulate material on the global cycles of the elements. Appl. Geochem. 26, S365–S369.
Oelkers, E.H., Gíslason, S.R., 2001. The mechanism, rate and consequences of basaltic glass dissolution: I. An experimental study of the dissolution rates of basaltic glass as a function of aqueous As, Si and oxalic acid concentration at 25°C and pH = 3 and 11. Geochim. Cosmochim. Acta 65, 3671–3681.
Oelkers, E.H., Valsami-Jones, E., Roncal-Herrero, T., 2008. Phosphate mineral reactivity: from global cycles to sustainable development. Mineral. Mag. 72 (1), 337–340.
Osborne, A.H., Haley, B.A., Hathorne, E.C., Flögel, S., Frank, M., 2014. Neodymium isotopes and concentrations in Caribbean seawater: tracing water mass mixing and continental input in a semi-enclosed ocean basin. Earth Planet. Sci. Lett. 406, 174–186.
Paul, S.A., Haeckel, M., Bau, M., Bajracharya, R., Koschinsky, A., 2019. Small-scale heterogeneity of trace metals including rare earth elements and yttrium in deep-sea sediments and porewaters of the Peru Basin, southeastern equatorial Pacific. Biogeosciences 16 (24), 4829–4849.
Pavia, F.J., Anderson, R.F., Winckler, G., Fleisher, M.Q., 2020. Atmospheric dust inputs, iron cycling, and biogeochemical connections in the South Pacific Ocean from thorium isotopes. Global Biogeochem. Cycles 34 (9). e2020GB006562.
Pearce, C.R., Jones, M.T., Oelkers, E.H., Pradoux, C., Jeandel, C., 2013. The effect of particulate dissolution on the neodymium (Nd) isotope and Rare Earth Element (REE) composition of seawater. Earth Planet. Sci. Lett. 369, 138–147.
Peucker-Ehrenbrink, B., 2009. Land2Sea database of river drainage basin sizes, annual water discharges, and suspended sediment fluxes. Geochem. Geophys. Geosyst. 10 (6).
Pilson, M.E., 2013. An Introduction to the Chemistry of the Sea. Cambridge University Press, Cambridge, UK.
Pin, C., Zalduegui, J.S., 1997. Sequential separation of light rare-earth elements, thorium and uranium by miniaturized extraction chromatography: application to isotopic analyses of silicate rocks. Anal. Chim. Acta 339 (1–2), 79–89.
Roberts, N.L., Piotrowski, A.M., 2015. Radiogenic Nd isotope labeling of the northern NE Atlantic during MIS 2. Earth Planet. Sci. Lett. 423, 125–133.
Roncal-Herrero, T., Rodríguez-Blanco, J.D., Oelkers, E.H., Benning, L.G., 2011. The direct precipitation of rhabdophane (REEPO $_4\cdot$ nH $_2$ O) nano-rods from acidic aqueous solutions at 5–100° C. J. Nanopart. Res. 13 (9), 4049.
Rousseau, T.C., Sonke, J.E., Chmeleff, J., Van Beek, P., Souhaut, M., Boaventura, G., Seyler, P., Jeandel, C., 2015. Rapid neodymium release to marine waters from lithogenic sediments in the Amazon estuary. Nat. Commun. 6, 7592.
Shabani, M.B., Akagi, T., Masuda, A., 1992. Preconcentration of trace rare-earth elements in seawater by complexation with bis (2-ethylhexyl) hydrogen phosphate and 2-ethylhexyl dihydrogen phosphate adsorbed on a C18 cartridge and determination by inductively coupled plasma mass spectrometry. Anal. Chem. 64 (7), 737–743.
Shiller, A.M., 2002. Seasonality of dissolved rare earth elements in the lower Mississippi River. Geochem. Geophys. Geosyst. 3 (11), 1–14.
Shiller, A.M., Joung, D., 2012. Nutrient depletion as a proxy for microbial growth in Deepwater Horizon subsurface oil/gas plumes. Environ. Res. Lett. 7, (4) 045301.
Sholkovitz, E.R., 1989. Artifacts associated with chemical leaching of sediments for rare-earth elements. Chem. Geol. 77, 47–51.
Sholkovitz, E.R., 1992. Chemical evolution of rare earth elements: fractionation between colloidal and solution phases of filtered river water. Earth Planet. Sci. Lett. 114 (1), 77–84.
Sholkovitz, E.R., 1995. The aquatic chemistry of rare earth elements in rivers and estuaries. Aquatic geochem. 1 (1), 1–34.
Sholkovitz, E., Szymczak, R., 2000. The estuarine chemistry of rare earth elements: comparison of the Amazon, Fly, Sepik and the Gulf of Papua systems. Earth Planet. Sci. Lett. 179 (2), 299–309.
Tanaka, T., Togashi, S., Kamioka, H., Amakawa, H., Kagami, H., Hamamoto, T., Yuhara, M., Orihashi, Y., Yoneda, S., Shimizu, H., Kunimaru, T., 2000. JNdi-1: a neodymium isotopic reference in consistency with LaJolla neodymium. Chem. Geol. 168 (3–4), 279–281.
Taylor, S.R., McLennan, S.M., 1985. The Continental Crust: Its Composition and Evolution. Blackwell Scientific, Boston, Mass.
Tessier, A., Campbell, P.G., Bisson, M., 1979. Sequential extraction procedure for the speciation of particulate trace metals. Anal. Chem. 51 (7), 844–851.
Tipping, E., Hetherington, N.B., Hilton, J., Thompson, D.W., Bowles, E., Hamilton-Taylor, J., 1985. Artifacts in the use of selective chemical extraction to determine distributions of metals between oxides of manganese and iron. Anal. Chem. 57 (9), 1944–1946.
Trefry, J.H., Shokes, R.F., 1981. History of heavy-metal inputs to Mississippi Delta sediments. *Elsevier Oceanography Series* 27, 193–208.
Viers, J., Dupré, B., Gaillardet, J., 2009. Chemical composition of suspended sediments in World Rivers: New insights from a new database. Sci. Total Environ. 407 (2), 853–868.
Walling, D.E., 2006. Human impact on land–ocean sediment transfer by the world's rivers. Geomorphology 79 (3–4), 192–216.
Wilkin, R.T., Ford, R.G., 2002. Use of hydrochloric acid for determining solid-phase arsenic partitioning in sulfidic sediments. Environ. Sci. Technol. 36 (22), 4921–4927.
Wilson, D.J., Piotrowski, A.M., Galy, A., Clegg, J.A., 2013. Reactivity of neodymium carriers in deep sea sediments: Implications for boundary exchange and paleoceanography. Geochim. Cosmochim. Acta 109, 197–221.

Supplementary Materials

Evolution of rare earth element and εNd compositions of Gulf of Mexico seawater during interaction with Mississippi River sediment

Segun B. Adebayo[a]*, Minming Cui[a, b], Thomas J. Williams[c], Ellen Martin[c], and Karen H. Johannesson[a, d].

[a] *Department of Earth and Environmental Sciences, Tulane University, New Orleans, LA 70118, USA*

[b] *Morton K. Blaustein Department of Earth and Planetary Sciences, Johns Hopkins University, Baltimore, MD 21218, USA*

[c] *Department of Geological Sciences, University of Florida, Gainesville, FL 32611, USA*

[d] *School for the Environment, University of Massachusetts Boston, Boston, MA 02125, and Intercampus Marine Science Graduate Program, University of Massachusetts System, Boston, MA 02125, USA*

*Corresponding author: email- sadebay@tulane.edu

1. Mississippi River Sediments

Table S1. The REE concentrations in the operationally defined "exchangeable" fraction of the Mississippi River sediments as reported by Adebayo *et al.* (2018).

Sediments REE concentrations (nmol kg^{-1})	
La	63 ± 10
Ce	265 ± 27
Pr	46 ± 4
Nd	327 ± 45
Sm	182 ± 9
Eu	84 ± 7
Gd	172 ± 13
Tb	
Dy	142 ± 10
Ho	44 ± 3
Er	145 ± 10
Tm	
Yb	140 ± 12
Lu	15 ± 1
HREE/LREE	8.66
Ce/Ce*	0.97
Eu/Eu*	2.62
Gd/Gd*	1.48

HREE/LREE is defined as $(Tm_N + Yb_N + Lu_N) / (La_N + Pr_N + Nd_N)$

Anomalies: $Ce/Ce^* = 2[Ce]_N/([La]_N+[Pr]_N)$; $Eu/Eu^* = 2[Eu]_N/(0.67[Sm]_N+0.33[Tb]_N)$; $Gd/Gd^* = [Gd]_N/(0.33[Sm]_N+0.67[Tb]_N)$

where $_N$ refers to shale-normalized values.

2. Sediment Characterization

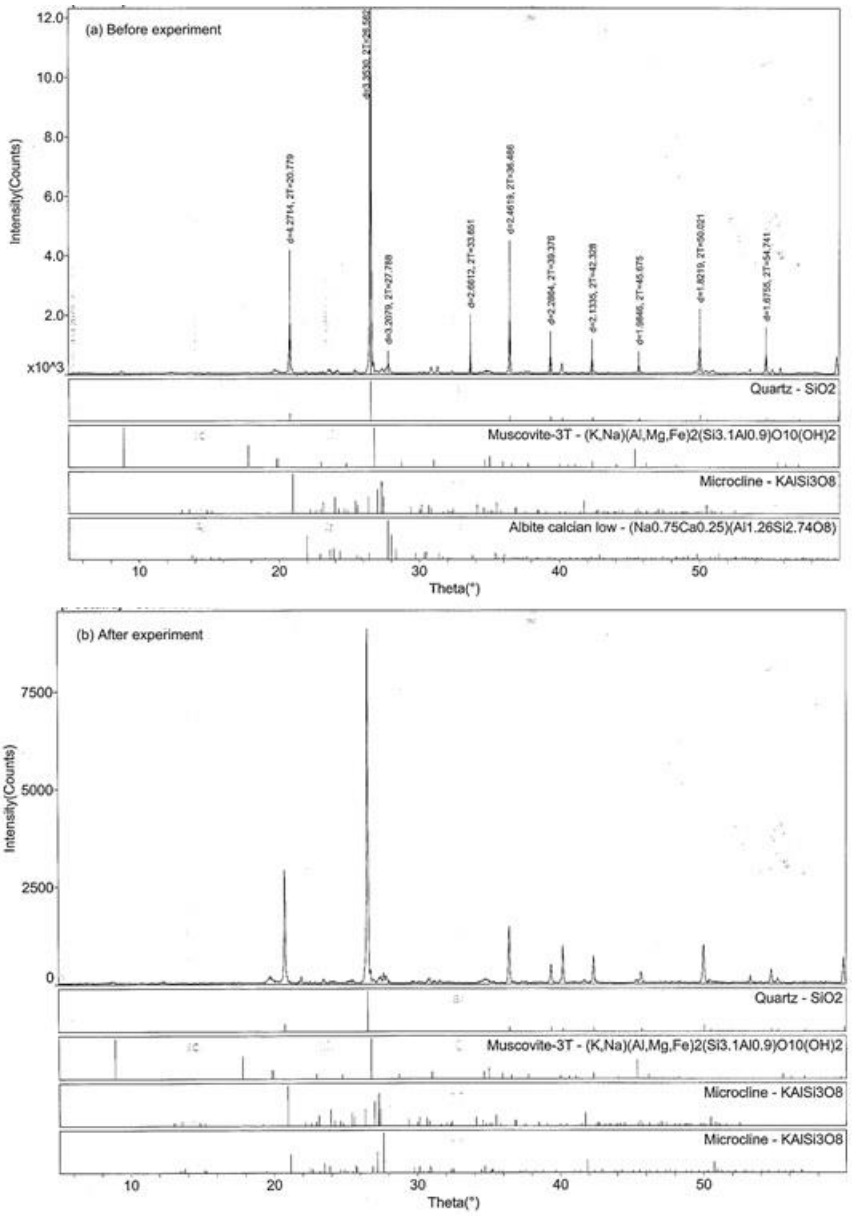

Figure S1. X-ray diffractograms of the Mississippi River sediments. Panel (a) shows the sample before, and panel (b) shows the sample after the batch reaction experiments.

3. REE Fractionation Pattern

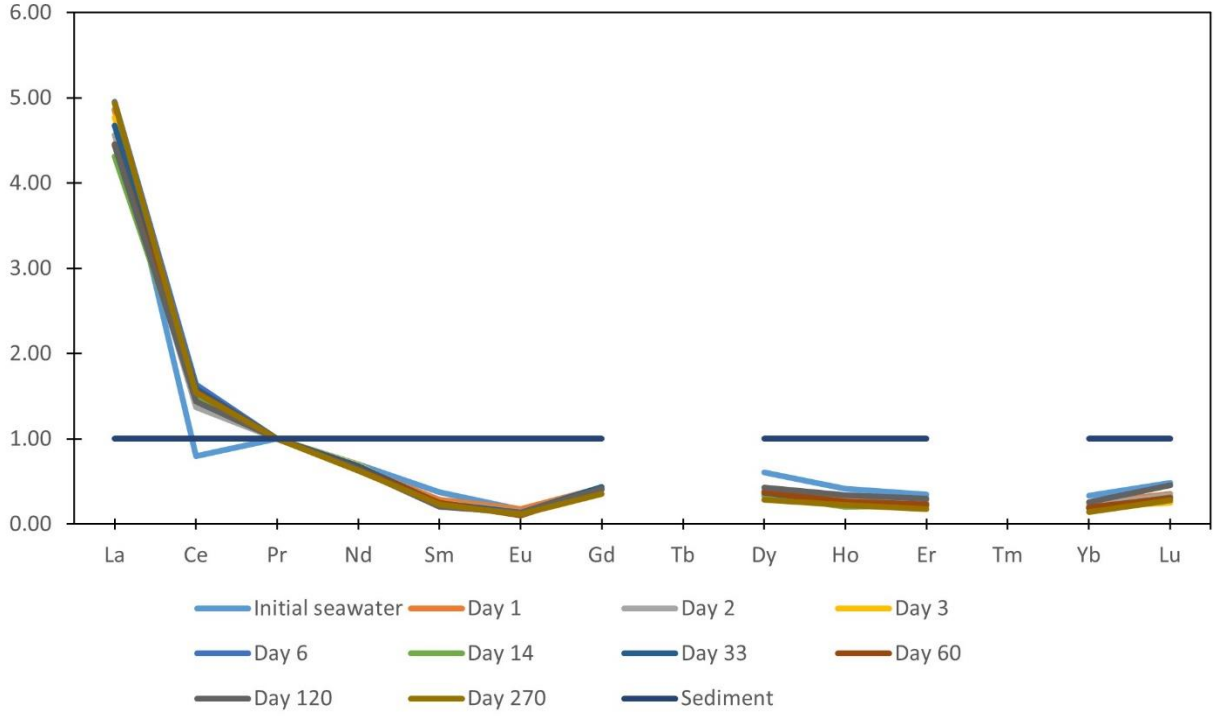

Figure S2. Dissolved REE concentrations in the reacted seawater normalized to the REE concentrations in the "exchangeable" fraction of the sediments and then again to the sediments-normalized Pr concentration to account for high variance in concentrations.

4. Geochemical Modeling

Geochemical modeling of the experimental solutions was achieved using the SpecE8 and React programs of the Geochemist's Workbench® (Release 14.0.1; Bethke *et al.,* 2020a, b). The Lawrence Livermore National Laboratory database (Delaney and Lundeen, 1989) provided with the Geochemist's Workbench® software (i.e., `thermo.tdat`) was modified by the addition of the 14 naturally occurring rare earth elements (REE) and their corresponding inorganic complexes with carbonate, bicarbonate, phosphate, hydroxyl, sulfate, chloride, and fluoride ions are described by Johannesson *et al.* (2017). Specifically, infinite dilution stability constants for the $LnHCO_3^+$, $LnCO_3^+$, and $Ln(CO_3)_2^-$ complexes, where Ln is any of the 14 naturally occurring REEs (i.e., lanthanides) that were added to the database are from Luo and Byrne (2004), those for $LnPO_4^0$ and $Ln(PO_4)_2^{3-}$ are from Byrne et al. (1991) and Lee and Byrne (1992), those for $LnOH^+$ are from Klungness and Byrne (2000), those for $LnSO_4^+$ are from Schijf and Byrne (2004), those for $LnCl^+$ are from Luo and Byrne (2001), and those for LnF^+ are from Luo and Byrne (2000). We also added the solubility product constants for $LnPO_{4(s)}$ phases that were

estimated by Liu and Byrne (1997) to the database. The new database containing the REEs is renamed `thermo_REE.tdat`.

Because we did not measure the major ion composition of the Gulf of Mexico seawater sample used in our experiments, we assumed a starting composition equivalent to that given in Pilson (2013) for our simulations. Because, except for carbonate ions, the ratios of the major ions in seawater varies by less than 1% in the ocean (e.g., Millero, 2006), the use of Pilson's (2013) major ion data is justified for a first-order model of the aqueous speciation of REEs in seawater, including our Gulf of Mexico sample. To model the impact of dissolved phosphate on REE speciation we used the phosphate concentration reported by Shiller and Joung (2012) for Gulf of Mexico seawater from the same depth as our seawater sample was collected.

Initially, we ran simple sliding activity reaction path models to investigate the impact of acidification and basification of the seawater sample. These simple reaction path models only show how the major anions would vary as pH is lowered from 8.1 to 2, and subsequently raised back to 8.1. Note that the models do not account for the extra Cl^- and Na^+ ions added in the acidification (using HCl) and basification (using NaOH) of the collected seawater sample prior to the batch experiments. We note that Cl^- only forms weak aqueous complexes with the REEs in low-temperature natural waters such as seawater and that Na^+ is perhaps the most conservative major metal cation in seawater (Millero, 1992). Chloride does form strong complexes with REEs in geothermal fluids (Haas et al., 1995).

An example script for the sliding pH models run with the React program is shown below

```
data thermo.tdat verify

# Major ion data are from Pilson (2013)
# Phosphate data for Gulf of Mexico from Shiller and Juong (2012)

Cl-      = 545.88 mmol/kg
Ca++     =  10.28 mmol/kg
Mg++     =  52.83 mmol/kg
Na+      = 468.96 mmol/kg
K+       =  10.21 mmol/kg
SO4--    =  28.23 mmol/kg
HCO3-    =   2.06 mmol/kg
HPO4--   =   1.0  umol/kg

pH       = 8.1

slide pH to 2.0

pickup reactants = fluids

slide pH to 8.1
```

It is important to note that HCO3-, HPO4--, Ca++ and so forth given in the script represent the model basis for the total dissolved inorganic carbonate, phosphate, calcium, etc., and not the specific concentrations of the HCO_3^-, HPO_4^{2-}, Ca^{2+} ions in solution (Bethke, 2008). Figure S3 shows the result of the acidification step (note, the results of the basification step is identical except for the direction of pH change.

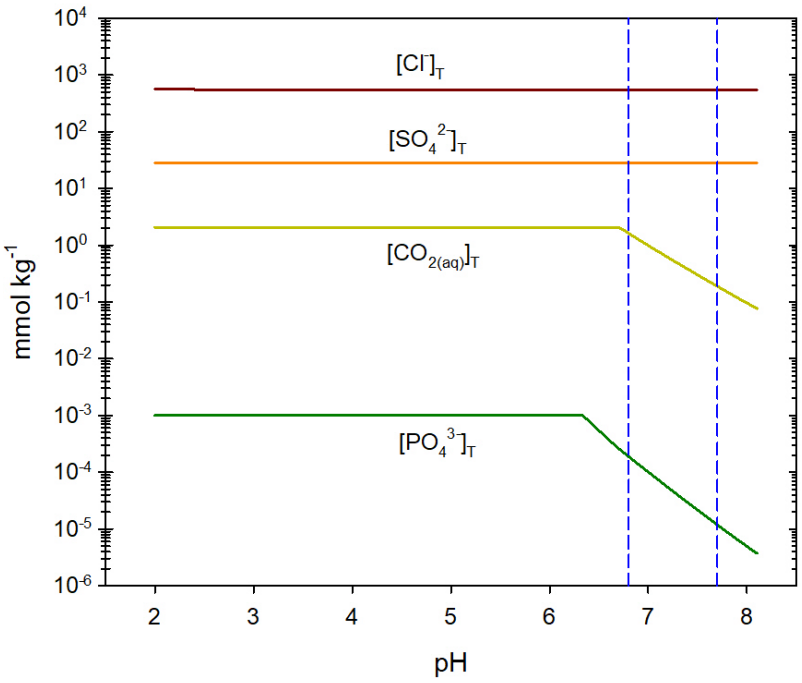

Figure S3. Results of simple sliding activity reaction path model for seawater from pH 8.1 to 2. Total dissolved chloride and sulfate vary only slightly, whereas both the total dissolved $CO_{2(aq)}$ and $PO_{4(aq)}$ increase. Note, that the vertical dashed blue lines show the pH range of our batch reactor experiments (i.e., $6.8 \leq pH \leq 7.7$)

The results of the simple sliding activity reaction path models for seawater suggest that the total chloride and sulfate concentrations will not change substantially over the pH range of our experiments ($6.8 \leq pH \leq 7.7$). However, changes are expected for total dissolved carbonate and phosphate. Figure 2 shows the results for individual carbonate and phosphate species as a function of pH.

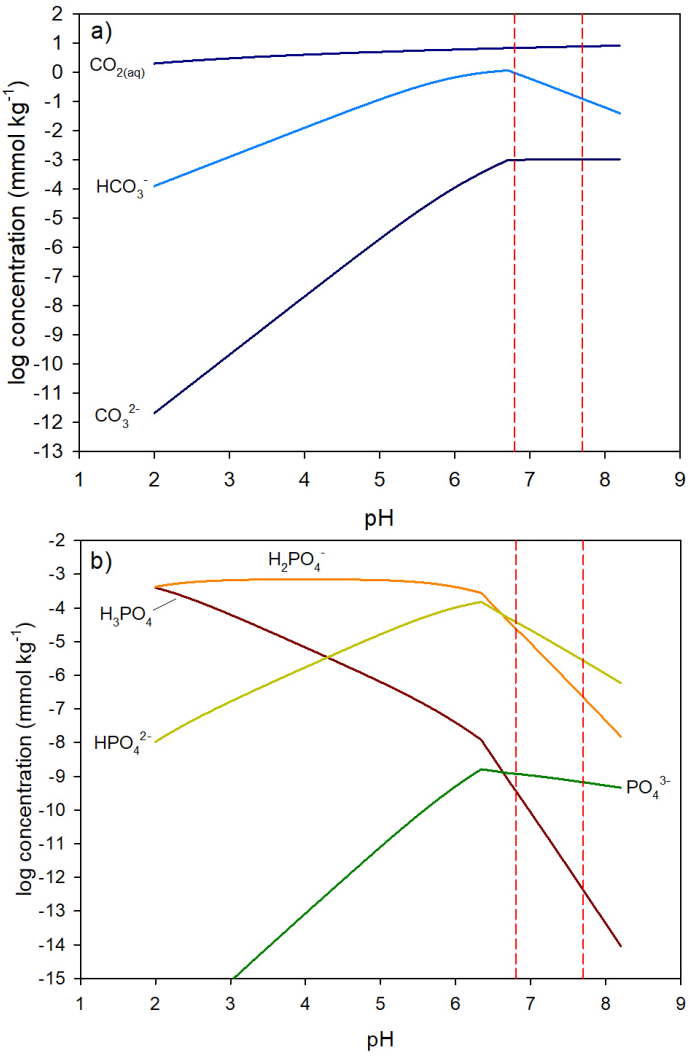

Figure S4. Speciation of inorganic carbonate and phosphate in seawater as a function of pH. The vertical, dashed red lines show the range of pH of our batch experiments (i.e., 6.8 ≤ pH ≤ 7.7). For this pH range, the concentrations of the CO_3^{2-} and PO_4^{3-} ions are predicted to be relatively constant compared to other carbonate ions (e.g., HCO_3^-) and phosphate species for the simplistic, sliding activity models.

To model the speciation of REEs in our batch experiments we first used the major ion composition of typical seawater from Pilson (2013) and slide the pH from 8.1 (pH of the seawater sample measured in the field) to the pH measured in each sacrificed batch reactor to adjust the major ion composition to values appropriate for the batch reactors' pH values. For example, the initial script for the React program employed for the batch reactor at Day 14 is given below:

```
data thermo.tdat verify

# Major ion data are from Pilson (2013)
# Phosphate data for Gulf of Mexico from Shiller and Juong (2012)
# Day 14 of batch experiments

Cl-      = 545.88 mmol/kg
Ca++     =  10.28 mmol/kg
Mg++     =  52.83 mmol/kg
Na+      = 468.96 mmol/kg
K+       =  10.21 mmol/kg
SO4--    =  28.23 mmol/kg
HCO3-    =   2.06 mmol/kg
HPO4--   =   1.0  umol/kg

pH       = 8.1

slide pH to 6.8
```

The results of the simulation were then employed to input the calculated major ion compositions as well as our measured REE concentrations into speciation scripts used with the SpecE8 model of the Geochemist's Workbench®. For example, the speciation script for Day 14 is given below:

```
data thermo_REE.tdat verify

# Major ion data are from Pilson (1998)
# Phosphate data for Gulf of Mexico from Shiller and Juong (2012)
# Day 14

Cl-      = 546.7  mmol/kg
Ca++     =  10.06 mmol/kg
Mg++     =  52.62 mmol/kg
Na+      = 469.0  mmol/kg
K+       =  10.21 mmol/kg
SO4--    =  28.23 mmol/kg
HCO3-    =   1.628 mmol/kg
HPO4--   =   1.0 umol/kg

pH       = 6.8
SiO2(aq) = 176.43 umol/kg

La+++   = 1302.0e-12 molal
Ce+++   = 1832.0e-12 molal
Pr+++   =  193.0e-12 molal
Nd+++   =  926.0e-12 molal
Sm+++   =  181.0e-12 molal
Eu+++   =   44.0e-12 molal
Gd+++   =  289.0e-12 molal
Tb+++   =   35.0e-12 molal
Dy+++   =  198.0e-12 molal
Ho+++   =   41.0e-12 molal
Er+++   =  130.0e-12 molal
Tm+++   =   18.0e-12 molal
Yb+++   =  109.0e-12 molal
Lu+++   =   19.0e-12 molal

balance on HCO3-

print species = long

print saturations = long
```

For the sensitivity testing, we varied the total dissolved phosphate concentrations from 0.5 µmol kg^{-1} to 1.5 µmol kg^{-1}, which captured the ranges of PO4 values observed during the simulations to investigate the impact of various phosphate concentrations on the saturation state of the batch reactor solutions with respect to $LnPO_{4(c)}$ phases. The results are shown in Figure S5 below:

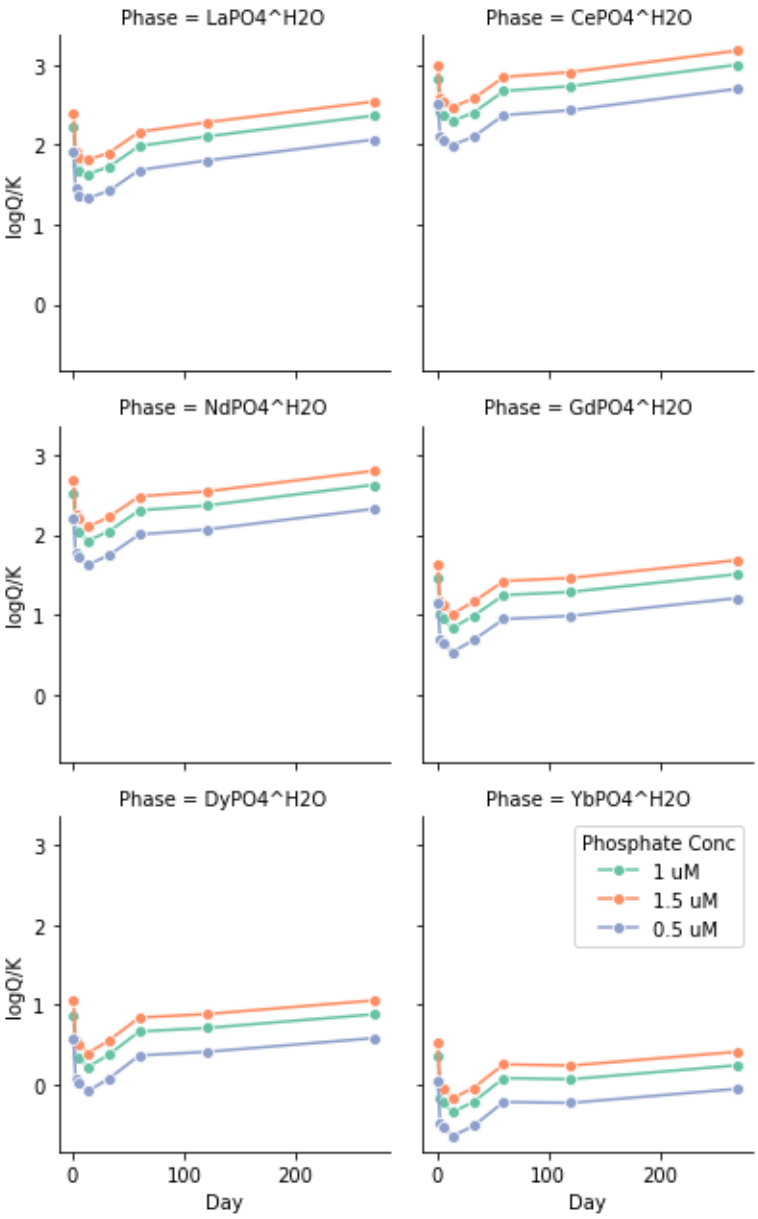

Figure S5. Modeled saturation indices for the batch reactor solutions with respect to secondary $LnPO_4 \bullet H_2O$ phases as a function of time and phosphate concentrations. All experimental solutions are oversaturated with respect to $LREEPO_4 \bullet H_2O$ phases for the entire experiment. $HREEPO_4 \bullet H_2O$ phases are oversaturated at the beginning of the experiment and after 33 days.

References

Adebayo, S. B., Cui, M., Hong, T., White, C. D., Martin, E. E., and Johannesson, K. H. (2018) Rare earth elements geochemistry and Nd isotopes in the Mississippi River and Gulf of Mexico mixing zone. *Frontiers in Marine Science*, ***5***, 166.

Bethke C. M. (2008) *Geochemical and Biogeochemical Reaction Modeling*, 2nd ed. Cambridge University Press, Cambridge, UK.

Bethke C. M., Farrell B., and Sharifi M. (2020a) *The Geochemist's Workbench® Release 14: GWB Essentials Guide.* Aqueous Solutions, LLC, Champaign, IL, 208 pp.

Bethke C. M., Farrell B., and Sharifi M. (2020b) *The Geochemist's Workbench® Release 14: GWB Reaction Modeling Guide*. Aqueous Solutions, LLC, Champaign, IL, 218 pp.

Byrne R. H., Lee J. H., and Bingler L. S. (1991) Rare earth element complexation by PO_4^{3-} ions in aqueous solutions. *Geochim. Cosmochim. Acta* **55**, 2729-2735.

Delaney J. M. and Lundeen S. R. (1989) The LNLL thermochemical database. Lawrence Livermore National Laboratory, Report UCRL-21658.

Haas J. R., Shock E. L., and Sassini D. C. (1995) Rare earth elements in hydrothermal systems: Estimates of standard partial molar thermodynamic properties of aqueous complexes of the rare earth elements at high pressures and temperatures. *Geochim. Cosmochim. Acta* **59**, 4329-4350.

Johannesson K. H., Palmore C. D., Fackrell J., Prouty N. G., Swarzenski P. W., Chevis D. A., Telfeyan K., White C. D., and Burdige D. J. (2017) Rare earth element behavior during groundwater–seawater mixing along the Kona Coast of Hawaii. *Geochim. Cosmochim. Acta* **198**, 229-258.

Klungness G. D. and Byrne R. H. (2000) Comparative hydrolysis behavior of the rare earth elements and yttrium: the influence of temperature and ionic strength. *Polyhedron* **19**, 99-107.

Lee J. H. and Byrne R. H. (1992) Examination of comparative rare earth element complexation behavior using linear free-energy relationships. *Geochim. Cosmochim. Acta* **56**, 1127-1137.

Liu X. and Byrne R. H. (1997) Rare earth and yttrium phosphate solubilities in aqueous solution. *Geochim. Cosmochim. Acta* **61**, 1625-1633.

Luo Y.-R. and Byrne R. H. (2000) The ionic strength dependence of rare earth and yttrium fluoride complexes as 25 ºC. *J. Sol. Chem*. **29**, 1089-1099.

Luo Y.-R. and Byrne R. H. (2001) Yttrium and rare earth element complexation by chloride ions at 25 ºC. *J. Sol. Chem*. **30**, 837-845

Luo Y.-R. and Byrne R. H. (2004) Carbonate complexation behavior of yttrium and the rare earth elements in natural waters. *Geochim. Cosmochim. Acta* **68**, 691-699.

Millero F. J. (1992) Stability constants for the formation of rare earth inorganic compleses as a function of ionic strength. *Geochim. Cosmochim. Acta* **56**, 3123-3132.

Millero F. J. (2006) *Chemical Oceanography*, 3rd ed. CRC Press, Boca Raton, FL.

Pilson M. E. Q. (2013) *An Introduction to the Chemistry of the Sea*, 2nd ed. Cambridge University Press, Cambridge, UK.

Schijf J. and Byrne R. H. (2004) Determination of $_{SO4}\beta_1$ for yttrium and the rare earth elements at I = 0.66 m and t = 25 °C – implications for YREE solution complexation in sulfate-rich waters. *Geochim. Cosmochim. Acta* **68**, 2825-2837.

Shiller A. M. and Joung D. (2012) Nutrient depletion as a proxy for microbial growth in Deepwater Horizon subsurface oil/gas plumes. Environ. Res. Lett. 7, 045301, doi:10.1088/1748-9326/7/4/045301.